Appendix 1

PATENT

IN THE UNITED STATES PATENT AND TRADEMARK OFFICE

In re Application of:
Yang, *et al.*

Serial No.: 10/732,919

Filed: December 10, 2003

For: N2S2 Chelate-Targeting Ligand Conjugates

Confirmation No. 7351

Group Art Unit: 1618

Examiner: Schlientz, Leah H.

Atty. Dkt. No.: UTSC:841US

CERTIFICATE OF ELECTRONIC TRANSMISSION
37 C.F.R. § 1.8

I hereby certify that this correspondence is being electronically filed with the United States Patent and Trademark Office via EFS-Web on the date below.

Aug. 28, 2009
Date

Monica A. De La Paz

I, Jerry Bryant, do declare that:

1. I am a United States citizen residing at 6861 Staffordshire St. Houston, TX 77030.

2. I currently hold the position of Chief Technology Officer, Head of Scientific Evaluation, Division of Business Development, Cell>Point, LLC, 7120 E. Orchard Road, Suite 350, Englewood, CO 80111. A copy of my curriculum vitae, including a list of my publications, is attached as Appendix A.

3. I am skilled in the synthesis and use of radionuclide-labeled imaging agents, as evidenced by the following:

- I have worked as Chief Technology Officer of Cell>Point, LLC since 2001.
- I have been employed as the Director of Research Development of VeriMed Research Corporation in Houston, TX, from 2002-2004.

APPENDIX 1

- My duties at Cell≫Point and VeriMed include participation in the development of novel radiopharmaceuticals for different diseases, such as cancer, cardiovascular disease, and diabetes. I have also been involved with studies directed to the synthesis and use of radionuclides, and studies directed to understanding the mechanism and biochemistry of the agents as it pertains to the pharmacokinetics and biodistribution of the agents in animals and humans. In addition, I have been involved in the evaluation of new technologies for the treatment of cancer, cardiovascular disease, and diabetes.
- I was employed as Chief Scientific Officer of Allcure, Inc., in Houston, TX, from May, 2001-May, 2002. My duties at Allcure included designing and marketing *in vitro* and *in vivo* services to drug and bio-tech companies for evaluating compounds of interest (nuclear medicine, SCID mouse *in vivo* service and mechanism studies).
- I have experience as a Research Assistant II in the Department of Nuclear Medicine, the Division of Diagnostic Imaging, of the University of Texas M.D. Anderson Cancer Center, from October, 2002 to June, 2003.
- I am a co-inventor of two patent applications that pertain to imaging technology, including USSN 10/703,405 ("Ethylenedicysteine (EC)-Drug Conjugates, Compositions, and Methods for Tissue Specific Disease Imaging," Yang *et al.*); and USSN 10/942,615 ("Mechanism-Based Targeted Pancreatic Beta Cell Imaging and Therapy," Yang *et al.*).
- I have been involved in funded studies pertaining to the development and evaluation of imaging agents during the past five years, including: (1) a study of CT and MRI functional agent development and evaluation supported by VeriMed Research Corporation; (2) a study of 99m-Tc-Ethylenedicysteine (EC)-Drug Conjugates for Tissue Specific Disease Imaging supported by Cell≫Point, LLC; and (3) a study to compare Tc-99m-EC-deoxyglucose (EC-DG) and FDG-PET scans for the evaluation of patients

suspected of having persistent/recurrent squamous cell carcinoma of the larynx after definitive treatment with radiation therapy and the evaluation of primary lung cancer patients, sponsored by Cell>Point, LLC. See page 7 of Appendix A.

- I am a co-author of seven articles and numerous abstracts pertaining to the evaluation and testing of radiolabeled imaging agents. See pages 9-14 of Appendix A.
- I am also a co-author of two book chapters pertaining to radiolabeled imaging agents and their uses in chemistry and nuclear medicine. See page 14 of Appendix A.
- Regarding my formal education, I have a Master of Science degree (1991) in Microbiology & Cell Science and Molecular Biology from the University of Florida, and a B.S. degree (1987) in Chemistry and Biochemistry from Tennessee State University.
- I have extensive experience in cell and molecular biology, as delineated in my curriculum vitae. See pages 2-3, Appendix A.

4. I have read the above-referenced patent application and the present Office Action, and am familiar with the technology. I understand that the examiner has rejected the claims because the examiner is of the opinion that at around November, 2002 when the application was filed, a person of ordinary skill in the field of the invention would have been motivated to substitute the ^{18}F-labeled penciclovir probe of Iyer *et al.* (J. Nucl. Med., 2001, 42, p. 96-105) with 99m-Tc-ethylenedicysteine (EC)-aminopenciclovir to practice the method of Iyer *et al.* to monitor expression of HSV1-thymidine kinase. The examiner argues that the teachings of Zareneyrizi *et al.* (Anti-Cancer Drugs, 1999, 10, p. 685-692) and Yang et al. (Ann. Nucl. Med. Sci., 2000, 13, p. 19-36) provide motivation to convert the penciclovir to amino penciclovir, and to label the aminopenciclovir with 99m-Tc-EC.

5. A person of ordinary skill in the art would not have been motivated to substitute the ^{18}F-labeled penciclovir probe of Iyer *et al.* with 99m-Tc-EC-aminopenciclovir because it is highly unlikely that 99m-Tc-EC-aminopenciclovir would be suitable for imaging HSV1-thymidine kinase reporter gene expression since it would not be a substrate for HSV1-thymidine kinase.

6. This is the case because the prior art teaches that the acyclic side chain of guanoside analogues such as penciclovir and acyclovir were known to substitute for sugar moieties. The side chain of Tc-EC-aminopenciclovir does not structurally resemble a sugar moiety or any part of a sugar moiety by virtue of the inclusion of the amino modification of penciclovir and by virtue of binding of EC (a molecule which does not structurally resemble a sugar moiety or part of a sugar moiety) to the amino moiety of aminopenciclovir. Information concerning the importance of structural similarity of the side chain to sugar moieties can be found, for example, in Elion *et al.*, Proc. Natl. Acad. Sci. USA, Vol. 74, No. 12, pp. 5716-5720, 1977 (Exhibit 1), Schaeffer *et al.*, J. Med. Chem. 14, 367-369, 1971 (Exhibit 2), and Schaeffer *et al.*, Nature, 1978 Apr 13;272(5654):583-5 (Exhibit 3).

7. Furthermore, a number of acyclic guanosine analogues were known in the field at the time of the filing date of the present patent application. These structural analogues were known to have acyclic side chains that include at least a portion of a sugar moiety. A number of references provided examples of acyclic guanosine analogues that were known to be substrates for HSV-thymidine kinase that have side chains resembling parts of sugar moieties, including De Clercq *et al.*, Nucleosides Nucleotides Nucleic Acids. 2001 Apr-Jul;20(4-7):271-85 (Exhibit 4), Ilsley *et al.*, Biochemistry. 1995 Feb 28;34(8):2504-10

(Exhibit 5), Golbraikh *et al.*, Nucleic Acids Res. 1989 Oct 11;17(19):7965-77 (Exhibit 5); and Martin *et al.*, J Med Chem. 1986 Aug;29(8):1384-9 (Exhibit 6).

8. Given this information concerning acyclic guanosine analogues that was known in the field, a person of ordinary skill in the field of the invention would not have been motivated to employ Tc-EC-aminopenciclovir in the method of Iyer et al. to probe for HSV1-thymidine kinase expression.

9. I hereby declare that all statements made herein of my knowledge are true and that all statements made on information and belief are believed to be true; and further that these statements were made with the knowledge that willful false statements and the like so made are punishable by fine or imprisonment, or both, under Section 1001 of Title 18 of the United States Code and that such willful false statements may jeopardize the validity of the application or any patent issued thereon.

8/5/2009
Date

Jerry Bryant

Appendix 2

PATENT

IN THE UNITED STATES PATENT AND TRADEMARK OFFICE

In re Application of:
Yang, *et al.*

Serial No.: 10/732,919

Filed: December 10, 2003

For: N2S2 CHELATE-TARGETING LIGAND CONJUGATES

Confirmation No. 7351

Group Art Unit: 1618

Examiner: Schlientz, Leah H.

Atty. Dkt. No.: UTSC:841US

CERTIFICATE OF ELECTRONIC TRANSMISSION
37 C.F.R. § 1.8

I hereby certify that this correspondence is being electronically filed with the United States Patent and Trademark Office via EFS-Web on the date below:

5/4/10
Date

Monica A. De La Paz

I, Jerry Bryant, do declare that:

1. I am a United States citizen residing at 6861 Staffordshire St. Houston, TX 77030.

2. I currently hold the position of Chief Technology Officer, Head of Scientific Evaluation, Division of Business Development, Cell>Point, LLC, 7120 E. Orchard Road, Suite 350, Englewood, CO 80111. A copy of my curriculum vitae and information concerning my expertise in the synthesis and use of radionuclide-labeled imaging agents, including a list of my publications, has previously been set forth in paragraph 2 and Appendix A of my first declaration (filed with the Patent Office on August 28, 2009). Cell>Point is a licensee of the technology of the present patent application.

3. I understand from the Office Action dated December 4, 2009 that the patent examiner is of the opinion that my previous declaration filed with the Patent Office on August 28,

2009 does not present sufficient proof that it is highly unlikely that ^{99m}Tc-EC-aminopenciclovir would be suitable for imaging HSV-1 thymidine kinase reporter gene expression since it would not be a likely substrate for HSV-1.

4. While I disagree with the Examiner's opinion that I have not provided sufficient proof to support my opinion, in an effort to provide clarification I will provide an even further detailed explanation to make it easier for the Examiner to understand why it is unlikely that ^{99m}Tc-EC-aminopenciclovir would be suitable for imaging HSV-1 thymidine kinase reporter gene expression.

5. By way of background, thymidine kinase catalyzes the transfer of a γ-phosphoryl moiety from ATP to 2'deoxythymidine (dThd) to produce thymidine 5'-monophosphate (dTMP) (reviewed in Tung and Summers, Amtimicrobial Agents and Chemotherapy, Sep. 1994, p. 2175-2179 (Exhibit A) and Omari *et al.*, BMC Structural Biology 2006, 6:22 (Exhibit B)). The reaction scheme is depicted in Exhibit C. As can be seen, thymidine kinase catalyzes the incorporation of a phosphate moiety at the 5-position of the deoxyribose moiety of thymidine.

6. The available literature at around the time of the filing date of the present patent application teaches that certain molecules that structurally resemble the natural substrate of thymidine kinase can undergo phosphorylation by thymidine kinase. Some of these molecules, such as penciclovir and acyclovir, include an acyclic side chain. The acyclic side chain includes hydroxyl moieties are positioned in a manner that resembles a portion of the deoxyribose moiety of thymidine and in particular that portion that includes the '5

hydroxyl moiety. FPCV is another such example. The hydroxyl moiety of the side chain of FPCV structurally resembles a portion of the deoxyribose moiety that includes a 5' hydroxyl moiety (see Exhibit D, which compares the acyclic moiety of FPCV to the deoxyribose moiety of thymidine).

7. 99m-Tc-EC-aminopenciclovir would not be expected by one of ordinary skill in the art to be suitable for imaging HSV1-thymidine kinase reporter gene expression because the available literature suggests that it would not be a good substrate for HSV-1 thymidine kinase. De Winter and Herdewijn (J Med Chem. 1996 Nov 22;39(24):4727-37; Exhibit E) teaches that molecules other than the natural substrate thymidine that are substrates of HSV-1 thymidine kinase are structurally strikingly similar to thymidine. See page 4727 left column and page 4733. 99m-Tc-EC-aminopenciclovir, with its bulky 99mTc-EC moiety and the amino group, is not structurally similar to thymidine. Further, De Winter and Herdewijn teaches that in designing high-affinity nucleoside substrates of HSV-1 thymidine kinase, "care should be taken to maintain the geometry of the base moiety and sugar hydroxyl functionalities." See abstract. A chemical drawing of ^{99m}-Tc-EC-aminopenciclovir is depicted in Exhibit F. In comparison to the chemical diagram of thymidine in Exhibit C, there is loss of a hydroxyl moiety relative to thymidine (and also relative to penciclovir). Thus, in 99m-Tc-EC-aminopenciclovir the geometry of sugar hydroxyl functionalities has clearly not been maintained. These findings are in contrast to FPCV, which does not include a bulky group attached to the acyclic moiety of FPCV and which maintains conformation of the hydroxyl group of the acyclic moiety in the 5' position.

8. In view of the above, a person of ordinary expertise in the synthesis and use of radionuclidie-labeled imaging agents would not have expected that ^{99m}Tc-EC-aminopenciclovir would be a suitable substrate for HSV1 thymidine kinase or a suitable agent for imaging HSV-1 thymidine kinase reporter gene expression.

9. I hereby declare that all statements made herein of my knowledge are true and that all statements made on information and belief are believed to be true; and further that these statements were made with the knowledge that willful false statements and the like so made are punishable by fine or imprisonment, or both, under Section 1001 of Title 18 of the United States Code and that such willful false statements may jeopardize the validity of the application or any patent issued thereon.

_____ _____

Date Jerry Bryant

Exhibit A

ANTIMICROBIAL AGENTS AND CHEMOTHERAPY, Sept. 1994, p. 2175–2179
0066-4804/94/$04.00+0

Vol. 38, No. 9

Substrate Specificity of Epstein-Barr Virus Thymidine Kinase

PETER P. TUNG[1] AND WILLIAM C. SUMMERS[1,2]*

Departments of Therapeutic Radiology[1] and Molecular Biophysics and Biochemistry, and Genetics,[2] Yale University School of Medicine, New Haven, Connecticut 06520-8040

Received 18 January 1994/Returned for modification 25 March 1994/Accepted 9 June 1994

Purified recombinant protein encoded by the BXLF-1 open reading frame of the Epstein-Barr virus genome has thymidine kinase activity. The substrate behaviors of various nucleosides toward this enzyme were tested. Halogenated deoxyuridines, zidovudine, and bromovinyldeoxyuridine are efficient substrates, while acyclovir and dihydroxypropylmethylguanine are relatively poor substrates for the Epstein-Barr virus thymidine kinase.

Like most other herpesviruses, Epstein-Barr virus (EBV) encodes a virus-induced protein with thymidine kinase (TK) activity. This enzyme catalyzes the transfer of the gamma phosphoryl group of ATP to the 5′ hydroxyl of a variety of deoxynucleosides to produce the corresponding nucleoside monophosphate. It is presumed that the further phosphorylations to the diphosphate and triphosphate forms are carried out by cellular kinases. In the case of herpes simplex virus type 1 (HSV-1) and HSV-2, the substrate specificity of the viral TK is much less restricted than that of the mammalian cell TK (12). Thus, in infected cells the viral enzyme initiates the conversion of nucleoside analogs to phosphorylated forms which either are inhibitors of the viral DNA polymerase or are relatively toxic when incorporated into the viral DNA (5). If the EBV TK has a similar broad substrate specificity, it may provide a route to the activation of nucleoside analogs for the production of useful antiviral nucleotides. To examine this possibility, we examined the use of various nucleoside analogs by EBV TK made in a bacterial expression system programed with the cloned EBV DNA sequence encoding this enzyme.

Reagents. Nucleoside analogs, thymidine, ATP, morpholinoethanesulfonic acid (MES), and bovine serum albumin (BSA) were purchased from Sigma. [^{14}C]thymidine and [γ-^{32}P]ATP were obtained from Amersham. [^{3}H]bromodeoxyuridine ([^{3}H]BrdU) was purchased from New England Nuclear. Water was from a Millipore MilliQ system. All other compounds were reagent grade or better.

EBV TK. The DNA sequence from nucleotides 144862 to 142745 of the B95-8 strain of EBV was cloned into the pET3a expression vector (20) at the *Nde*I and *Bam*HI sites. This vector was introduced into *Escherichia coli* SY 211 (25), a TK-deficient derivative of *E. coli* BL21 (DE3) (20), so that the only TK activity in the cell comes from the expression of the EBV sequences. Cultures were grown at 22°C in 4 liters of LB medium containing 200 μg of ampicillin per ml. Once the cultures reached the mid-log phase of growth, isopropylthiogalactoside was added to 0.4 mM to induce the expression of EBV TK. Induction was allowed to continue for 16 h at 22°C. Twenty grams (wet weight) of cells was harvested, washed with STE (20 mM NaCl, 1 mM EDTA, 10 mM Tris [pH 8.0]), and resuspended in 50 ml of 10% sucrose–50 mM Tris-HCl (pH 7.5) before being frozen in liquid nitrogen. The frozen cells were defrosted in 100 ml of 10% sucrose–200 mM NaCl–30 mM spermidine-HCl (pH 7.5) and were lysed by the addition of 300 μg of lysozyme per ml. The lysed cells were sonicated briefly to reduce the viscosity before pelleting the cellular debris. The supernatant was loaded directly onto a DEAE Biogel column (4 by 30 cm), and the column was eluted with 1 liter of a linear gradient of salt (0 to 500 mM NaCl). Fractions (6 ml) were collected and assayed for TK activity (see below). Fractions containing TK activity were pooled and applied to a hydroxylapatite column (1 by 8 cm) equilibrated with 1 mM potassium phosphate buffer (pH 6.8). The column was washed in succession with one column volume of the equilibrating buffer, the equilibrating buffer containing 500 mM NaCl, and finally the equilibrating buffer. The column was eluted with a 100-ml linear gradient of 10 to 300 mM potassium phosphate (pH 6.8) (10). Fractions with TK activity were dialyzed against 0.2 mM thymidine–50% glycerol–50 mM Tris (pH 6.8) and were stored at −20°C. The enzyme was judged to be about 30% pure on the basis of the staining intensity of the TK polypeptide on polyacrylamide gels.

Standard TK assay. Enzyme activity was determined by the differential binding of phosphorylated versus unphosphorylated nucleoside to positively charged DEAE paper (26). All assays were stopped prior to the consumption of greater than 5% of the substrate to ensure the linearity of the assay.

Assay for inhibition by competition. To assess the binding of nucleoside analogs to the TK, cold nucleoside analogs were used to compete with [^{14}C]thymidine as a substrate. To the reaction mixture was added 2 mM unlabeled nucleoside analog. The concentrations of the other reagents were kept the same. The assay conditions were identical to those described above for the standard TK assay; in particular, thymidine was present at 0.2 mM.

P transfer assay. Phosphorylation of the nucleoside analogs was determined by the transfer of radioactive phosphate from [γ-^{32}P]ATP to the nucleoside. This assay was performed as described by Doberson and Greer (8). The specific activity of [^{32}P]ATP used in these assays was 18 μCi/mmol.

The open reading frame from nucleotides 144861 to 143038 on the EBV genome (BXLFI) has previously been identified as having some homology to the HSV-1 and HSV-2 TK genes and, hence, is likely to encode an EBV TK (3). As predicted, the expression of this open reading frame yielded a polypeptide of about 70 kDa. This protein was found to aggregate in concentrated solutions and in low-ionic-strength buffers, making purification difficult. In this respect the recombinant enzyme behaved similarly to the TK activity from induced, EBV-containing lymphoblastoid cells (7). Gel filtration of the soluble form supported the conclusion that the enzyme exists in solution as a monomer of the expected size.

* Corresponding author. Mailing address: Department of Therapeutic Radiology, Yale University School of Medicine, P.O. Box 204000, New Haven, CT 06520. Phone: (203) 785 2986. Fax: (203) 785 6309. Electronic mail address: summers@biomed.med.yale.edu.

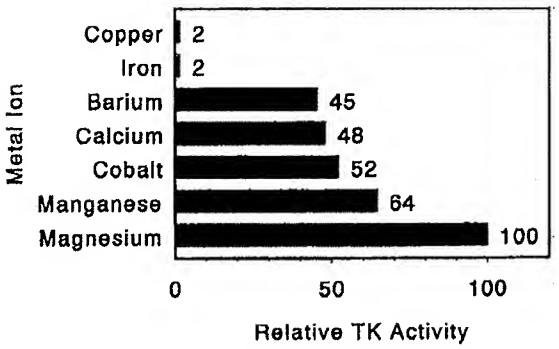

FIG. 1. Metal ion usage by EBV TK. No activity was observed in the absence of metal ions. Assay conditions were 10 mM metal chloride, 0.2 mM [^{14}C]thymidine (0.05 Ci/mM), 10 mM ATP, 0.6 mg of BSA per ml, and 100 mM MES (pH 6.0).

Initial characterization of the EBV TK activity was directed at determining the divalent metal ion requirements and the optimal pH for TK activity. EBV TK can use a variety of metals, with magnesium providing optimal activity (Fig. 1). Copper and iron are ineffective, while barium, calcium, cobalt, and manganese provide roughly the same activities. For subsequent study of substrate affinity, magnesium was the divalent ion used.

The apparent affinities of the EBV TK for the thymidine and ATP substrates were determined by measuring the reaction velocity as a function of each substrate concentration in the presence of an excess of the other. Lineweaver-Burk plots for both thymidine and ATP were linear (Fig. 2). This result suggests that the enzyme can be described by the simple

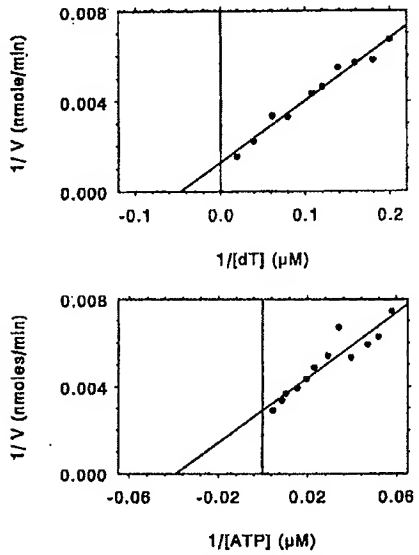

FIG. 2. Lineweaver-Burk plots varying dT and ATP. The K_m values obtained were 22 μM for dT and 25 μM for ATP.

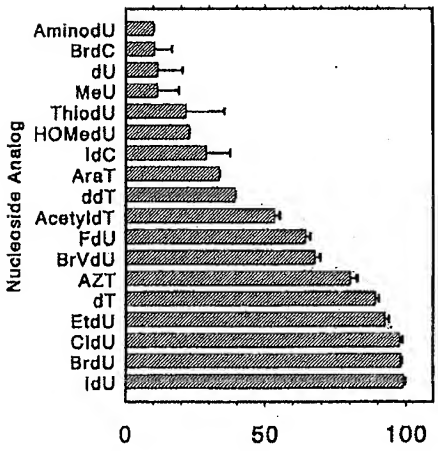

FIG. 3. Inhibition of EBV TK activity by nucleoside analogs measured by competition with thymidine. Assay conditions are described in the text.

Michaelis-Menten model for enzyme behavior. The apparent K_m for thymidine is 22 μM, and that for ATP is 25 μM.

Competition assays between nucleoside analogs and radiolabeled thymidine showed that a variety of nucleoside analogs can compete with thymidine for EBV TK (Fig. 3). Several 5-halogenated deoxyuridine analogs (5-chlorodeoxyuridine [CldU], BrdU, and 5-iododeoxyuridine [IdU]) appear to be even more effective competitors than the normal substrate thymidine. Although these comparisons are not as quantitatively precise as complete K_m/K_i determinations, they allow preliminary estimations of the potential usefulness of a given analog as an alternate substrate by the EBV TK. Since the molar ratio of the test compound to [^{14}C]thymidine was 10:1, this experimental approach is most informative for inhibitors which compete well with thymidine.

To test if the competitive analogs were able to function as alternate substrates and not just as inhibitors of true substrate binding, we examined the formation of phosphorylated product by using the appearance of new ^{32}P-labeled material as the basis for such activity. This assay is able to detect agents which are relatively efficiently phosphorylated; very low levels of phosphorylation may be masked by the unavoidable background of radioactive material which appears even in the absence of enzymatic activity. The following compounds exhibited detectable competition at concentrations 10-fold greater than the [^{14}C]thymidine concentration: 5′-aminodeoxyuridine (aminodU), 5-bromodeoxycytidine (BrdC), deoxyuridine (dU), methyluridine (meU), 4-thiodeoxyuridine (thiodU), 5-hydroxymethyldeoxyuridine (HOmedU), 5-iododeoxycytidine (IdC), thymine arabinofuranoside (araT), dideoxythymidine (ddT), 3′-*O*-acetylthymidine, (acetyldT), 5-fluorodeoxyuridine (FdU), 5-bromovinyldeoxyuridine (BrVdU), zidovudine (AZT), 5-ethyldeoxyuridine (EtdU), CldU, BrdU, and IdU (Fig. 3). All of these competitive nucleoside analogs were also phosphorylated by EBV TK. The following nucleoside analogs were not recognized by EBV TK: deoxyribosyladenine (dA), deoxyribosylcytidine (dC), deoxyribosylguanine (dG), α-deoxythymidine (αdT), 2-deoxyribose, 5′-aminodeoxythymidine, azadeoxycytidine, dihydroxypropylmethylguanine (DHPG), acyclovir, and

TABLE 1. Comparisons of dA, dC, and dG with thymidine as competitors and substrates for the EBV TK[a]

Nucleoside	cpm in:	
	Competition assay	Phosphorylation assay
None	1,002	890
dT	190	3,777
dA	1,053	636
dC	1,259	647
dG	1,086	623

[a] For the competition assay each nucleoside was added to the standard assay reaction mixture at a 10-fold molar excess over the ^{14}C-labeled thymidine substrate. For the phosphorylation assay, the production of phosphorylated nucleoside was assayed by the amount of ^{32}P transferred from ATP to the indicated nucleoside.

dideoxycytidine. They were neither competitive with thymidine nor phosphorylated. The data for dA, dC, and dG are presented in Table 1.

The substrate behavior of BrdU was analyzed in more detail (Fig. 4). [^{3}H]BrdU was used in place of [^{14}C]thymidine to assay enzyme activity, and these results confirm the fact that EBV TK phosphorylates BrdU. With a measured K_m of 15 μM for BrdU, EBV TK may have a slightly higher affinity for the nucleoside analog BrdU than for its presumptive natural substrate thymidine.

TK provides the pathway for phosphorylating various nucleoside analogs important in the treatment of herpes simplex virus (6) and human immunodeficiency virus. We characterized some aspects of EBV TK with an emphasis on its ability to use various nucleoside analogs. The requirement for a divalent metal ion is typical of most ATP-requiring enzymes since most such enzymes recognize Mg^{2+}-ATP as the physiological substrate (18). Since, except for Mg^{2+}, only one concentration of metal ion was examined in our survey, we cannot be sure that we have determined the optimal activity; we can be sure only that the metals tested function to some extent.

Linear double-reciprocal plots were obtained for both thymidine and ATP. This result indicates that EBV TK exhibits Michaelis-Menten kinetic behavior. For EBV TK the K_m for thymidine is 22 μM, while for HSV-1 TK the K_m is in the 0.5 μM range (5). Conversely, ATP binding is tighter for EBV TK,

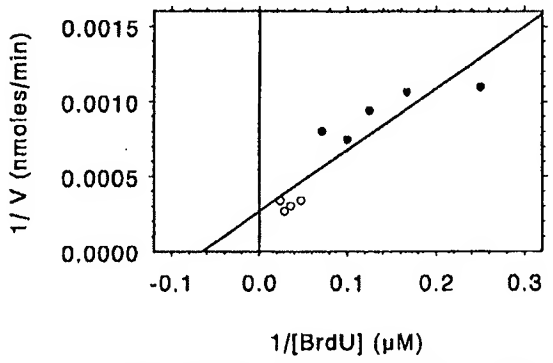

FIG. 4. Lineweaver-Burk plot varying BrdU. The K_m value obtained was 15 μM. Assay conditions were 10 mM NaF, 10 mM $MgCl_2$, 10 mM ATP, 0.6 mg of BSA per ml, 100 mM MES (pH 6.0), and various concentrations of [^{3}H]BrdU (0.1 to 0.2 Ci/mM). Data from two separate experiments are plotted as open and closed circles.

with a K_m of 25 μM, as opposed to a K_m of greater than 100 μM for HSV-1 TK. Since the intracellular pool concentration of thymidine is lower (21) than the K_m of the EBV TK, this pathway probably is of minor importance except during times of lytic viral replication when the cellular DNA may be degraded, raising the thymidine concentration.

It is interesting that, on the basis of the amino acid sequence homology, EBV TK and HSV TK have more homologous ATP-binding sites than thymidine-binding sites (3, 17). HSV TK is known to function also as a thymidylate kinase (4), and it will be interesting to see in further studies if EBV TK, purified to homogeneity to eliminate the possibility of contaminating proteins, has such an activity.

As shown in Fig. 3 it is apparent that a variety of nucleoside analogs are used by EBV TK. Changes in the base or changes in the sugar of the nucleoside can be accommodated by this TK. On the basis of the competitive activities of these analogs, we can infer that there are regions of the nucleosides in which structural modifications can be tolerated without destroying substrate-binding activity. Substitution on the sugar is tolerated at the 3′ position, with the bulkiness and charge of the group possibly determining the acceptability by the enzyme (compare AZT with acetyldT). Interestingly, ddT with a hydrogen substituted at the 3′ position is not as effective a substrate as AZT or acetyldT, which have much bulkier constituents. Only the substituents azide and acetyl, however, can function as hydrogen bond acceptors. This H bonding may be more important in TK substrate recognition than steric occupation.

The 2′ position of the sugar may also be substituted, although with limited acceptance by the TK. The ribose of methyl uridine and the arabinose of araT were both phosphorylated. Limited phosphorylation of araT by EBV TK indicates that the enzyme can distinguish the 2′ hydroxyl group in the beta orientation of the arabinose sugar.

Large changes in the nucleobase were least well tolerated. EBV TK only binds and phosphorylates pyrimidines. Of the naturally occurring nucleosides, thymidine is the best substrate, with some activity seen with deoxyuridine and no activity observed for dC. TK is thus dissimilar to HSV TK, which can phosphorylate most pyrimidines and some purines. However, Stinchcombe and Clough (23) reported that an activity in a DEAE column fraction, which seemed to be specific to lymphoblastoid cell lines expressing EBV lytic cycle genes, phosphorylated dC as efficiently as it did dT. Likewise, Littler and colleagues (17) have reported the ability of EBV TK to phosphorylate both deoxypyrimidines and deoxypurines. The purine analogs acyclovir and DHPG were also phosphorylated at a very low level in the preparation of EBV TK described by Littler et al. (17). Since the enzyme used by Stinchcombe and Clough (23) was an impure preparation isolated from lymphoblastoid cells in culture, it may have contained several different activities, some of which were unrelated to EBV yet which may have modulated the substrate behavior of the EBV TK polypeptide or altered its stability in some way. Although our observations, too, are based on only partially purified EBV TK, such other contaminating activities may have been eliminated from our preparation or may be absent from material produced from recombinant genes in *E. coli*. Another possibility to explain the discrepancy between our results and those of Stinchcombe and Clough (23) may be the phosphorylation of dC by a virus-induced kinase analogous to the cytomegalovirus protein kinase which can use dC as an alternate substrate (16, 24).

Deoxyuridines substituted at the 5 position were effectively used by the enzyme. Substituents at this position ranged from

vinyl to halogenated compounds. The chloro, bromo, and iodo 5-substituted deoxyuridines were the most effective nucleoside analogs and were better even than the physiological substrate thymidine. A comparison of the van der Waals radii suggests that these halogens (Cl = 0.18 nm, Br = 0.195 nm, I = 0.215 nm) are very close in size to the methyl of thymidine (0.20 nm). On the basis of steric factors, these analogs should bind as effectively as thymidine. With a somewhat smaller size, FdU (0.135 nm) was the least effective competitor among this series of 5-halodeoxyuridine analogs. However, the bromovinyl substituent is tolerated despite its larger size. The terminal bromomethene group on BrVdU may be oriented away from the active site and the proximal methene group may be situated to interact with the active-site pocket. This orientation would make BrVdU sterically similar to dT. A similar argument can be made for the proximal methene group of EtdU.

Hydrogen bonding at the active site may also play an important role in substrate recognition. Because of the electronegativities of the halogens, their effects on the nucleobase are to favor the enol tautomer as opposed to the keto tautomer favored by all other nucleobases, including thymidine (9). Such a change in hydrogen-binding potential, along with steric factors, may provide augmented binding in the active site and result in a substrate with a higher affinity than that of the naturally occurring one. That electronegativity alone is insufficient to explain our results, however, was shown in the case of the fluoro derivative, which, although it was the most electronegative, was a poor substrate. The steric effect in the case of the fluoropyrimidines may negate the increase in H bonding potential.

ACV has been reported to inhibit EBV replication in cell culture (13, 15) and has been used to treat EBV infections in a number of different clinical settings (1, 11). Our observations of the inability of EBV TK to phosphorylate this nucleoside analog are not incompatible with these findings. Although several studies have shown that ACV is inefficiently phosphorylated by cellular or virus-induced enzymes (14, 22), the action of ACV as a DNA chain terminator means that even very low levels of phosphorylation can be effective in stopping DNA replication. This interpretation is compatible with the literature reports of ACV efficiently inhibiting the production of EBV in culture and human patients while at the same time being poorly phosphorylated. While the clinical use of ACV has shown some success in the case of oral hairy leukoplakia, an EBV-related condition, other sorts of EBV infections have been reported to be resistant to treatment with ACV (2, 19, 27).

In summary, we characterized some aspects of EBV TK function, including the use of various nucleoside analogs to functionally probe the enzyme's active site. Understanding of the active site of this enzyme will allow a better understanding of the enzyme's mechanism of action and, in turn, the design of better substrate analogs with possible therapeutic importance.

This work was partially supported by NIH grants PO1-GM 39546 and PO1-CA 39238. Peter P. Tung was partially supported by NIH postdoctoral training grant T32-09159.

REFERENCES

1. **Andersson, J., S. Britton, I. Ernberg, U. Andersson, W. Henle, B. Skoldenberg, and A. Tisell.** 1986. Effect of acyclovir on infectious mononucleosis: a double-blind, placebo-controlled study. J. Infect. Dis. **153**:283–290.
2. **Andersson, J., and I. Ernberg.** 1988. Management of Epstein-Barr virus infections. Am. J. Med. **85**:107–115.
3. **Baer, R., A. T. Bankier, M. D. Biggin, P. L. Deininger, P. J. Farrell, T. J. Gibson, G. Hatfull, G. S. Hudson, S. C. Satchwell, C. Seguin, P. S. Tuffnell, and B. G. Barrell.** 1984. DNA sequence and expression of the B95-8 Epstein-Barr virus genome. Nature (London) **310**:207–211.
4. **Chen, M. S., J. Walker, and W. H. Prusoff.** 1979. Kinetic studies of herpes simplex virus type I-encoded thymidine and thymidylate kinase, a multifunctional enzyme. J. Biol. Chem. **254**:10747–10753.
5. **Cheng, Y. C.** 1976. Deoxythymidine kinase induced in HeLa TK^- cells by herpes simplex virus type I and type 2. II. Substrate specificity and substrate behaviours. Biochim. Biophys. Acta **452**: 370–381.
6. **Cheng, Y.-C., G. Dutschman, J. J. Fox, K. A. Watanabe, and H. Machida.** 1981. Differential activity of potential antiviral nucleoside analogs on herpes simplex virus-induced and human cellular thymidine kinases. Antimicrob. Agents Chemother. **20**:420–423.
7. **De Turenne-Tessier, M., T. Ooka, G. de The, and J. Daillie.** 1986. Characterization of an Epstein-Barr virus-induced thymidine kinase. J. Virol. **57**:1105–1112.
8. **Doberson, M. J., and S. Greer.** 1975. An assay for pyrimidine deoxyribonucleoside kinase using gamma-^{32}P-labeled ATP. Anal. Biochem. **67**:602–610.
9. **Freese, E.** 1959. The specific mutagenic effect of base analogues on phage T4. J. Mol. Biol. **1**:87–105.
10. **Gorbunoff, M. J.** 1985. Protein chromatography on hydroxyapatite columns. Methods Enzymol. **117**:370–380.
11. **Greenspan, D., Y. G. De Souza, M. A. Conant, H. Hollander, S. K. Chapman, E. T. Lennette, V. Peterson, and J. S. Greenspan.** 1990. Efficacy of desciclovir in the treatment of Epstein-Barr virus infection in oral hairy leukoplakia. J. Acquired Immune Defic. Syndr. **3**:571–578.
12. **Jamieson, A., G. A. Gentry, and J. H. Subak-Sharpe.** 1974. Induction of both thymidine and deoxycytidine kinase activity by herpes viruses. J. Gen. Virol. **24**:430–434.
13. **Lin, J. C., and H. Machida.** 1988. Comparison of two bromovinyl nucleoside analogs, 1-β-D-arabinofuranosyl-*E*-5-(2-bromovinyl) uracil and *E*-5-(2-bromovinyl)-2′-deoxyuridine, with acyclovir in inhibition of Epstein-Barr virus replication. Antimicrob. Agents Chemother. **32**:1068–1072.
14. **Lin, J.-C., D. J. Nelson, C. U. Lambe, and E. I. Choi.** 1986. Metabolic activation of 9([2-hydroxy-1-(hydroxymethyl)ethoxy] methyl)guanine in human lymphoblastoid cell lines infected with Epstein-Barr virus. J. Virol. **60**:569–573.
15. **Lin, J.-C., M. C. Smith, and J. S. Pagano.** 1985. Comparative efficacy and selectivity of some nucleoside analogs against Epstein-Barr virus. Antimicrob. Agents Chemother. **27**:971–973.
16. **Littler, E., A. D. Stuart, and M. Chee.** 1992. Human cytomegalovirus *UL97* open reading frame encodes a protein that phosphorylates the antiviral nucleoside analogue ganciclovir. Nature (London) **358**:160–162.
17. **Littler, E., J. Zeuthen, A. A. McBride, E. Trost-Sorensen, K. L. Powell, J. E. Walsh-Arrand, and J. R. Arrand.** 1986. Identification of an Epstein-Barr virus-coded thymidine kinase. EMBO J. **5**: 1959–1966.
18. **Phillips, R. C., P. George, and R. J. Rutman.** 1966. Thermodynamic studies of the function and ionization of the Mg(II) complexes of ADP and ATP over the pH range 5 to 9. J. Am. Chem. Soc. **88**:2631–2640.
19. **Pirsch, J. D., R. J. Stratta, H. W. Sollinger, G. R. Hafez, A. M. D'Alessandro, A. M. Kalayoglu, and F. O. Belzer.** 1989. Treatment of severe Epstein-Barr virus-induced lymphoproliferative syndrome with ganciclovir: two cases after solid organ transplantation. Am. J. Med. **86**:241–244.
20. **Rosenberg, A. H., B. N. Lade, D.-S. Chui, S.-W. Lin, J. J. Dunn, and F. W. Studier.** 1987. Vectors for selective expression of cloned DNAs by T7 RNA polymerase. Gene **56**:125–135.
21. **Sjostrom, D. A., and D. R. Forsdyke.** 1973. Isotope-dilution analysis of rate-limiting steps and pools affecting the incorporation of thymidine and deoxycytidine into cultured thymus cells. Biochem. J. **138**:253–262.
22. **Smee, D. F., R. Boehme, M. Chernow, B. P. Binko, and T. R. Mathews.** 1985. Intracellular metabolism and enzymatic phosphorylation of 9-(1,3-dihydroxy-2-propoxymethyl)guanine and

acyclovir in herpes simplex virus-infected and uninfected cells. Biochem. Pharmacol. 34:1049–1056.
23. **Stinchcombe, T., and W. Clough.** 1985. Epstein-Barr virus induces a unique pyrimidine deoxynucleoside kinase activity in superinfected and virus-producer B cell lines. Biochemistry 24:2027–2033.
24. **Sullivan, V., C. L. Talarico, S. C. Stanat, M. Davis, D. M. Coen, and K. K. Biron.** 1992. A protein kinase homologue controls phosphorylation of ganciclovir in human cytomegalovirus-infected cells. Nature (London) 358:162–164.
25. **Summers, W. C., and P. Raksin.** 1993. A method for selection of mutations at the *tdk* locus in *Escherichia coli*. J. Bacteriol. 175: 6049–6051.
26. **Summers, W. P., M. Wagner, and W. C. Summers.** 1975. Possible peptide chain termination mutants in thymidine kinase gene of a mammalian virus, herpes simplex virus. Proc. Natl. Acad. Sci. USA 72:4081–4084.
27. **Yao, Q. Y., P. Ogan, M. Rowe, M. Wood, and A. B. Rickenson.** 1989. The Epstein-Barr virus: host balance in acute infectious mononucleosis in patients receiving acyclovir anti-viral therapy. Int. J. Cancer 43:61–66.

Exhibit B

BMC Structural Biology

BioMed Central

Research article

Open Access

Structure of vaccinia virus thymidine kinase in complex with dTTP: insights for drug design

Kamel El Omari[1], Nicola Solaroli[2], Anna Karlsson[2], Jan Balzarini[3] and David K Stammers*[1]

Address: [1]Division of Structural Biology, The Wellcome Trust Centre for Human Genetics, University of Oxford, Oxford OX3 7BN, UK, [2]Karolinska Institute, Huddinge University Hospital, S-141 86, Stockholm, Sweden and [3]Rega Institute for Medical Research, K.U. Leuven, B-3000 Leuven, Belgium

Email: Kamel El Omari - kamel@strubi.ox.ac.uk; Nicola Solaroli - nicola.solaroli@ki.se; Anna Karlsson - anna.karlsson@ki.se; Jan Balzarini - Jan.Balzarini@rega.kuleuven.be; David K Stammers* - daves@strubi.ox.ac.uk

* Corresponding author

Published: 24 October 2006

BMC Structural Biology 2006, **6**:22 doi:10.1186/1472-6807-6-22

Received: 17 August 2006
Accepted: 24 October 2006

This article is available from: http://www.biomedcentral.com/1472-6807/6/22

Abstract

Background: Development of countermeasures to bioterrorist threats such as those posed by the smallpox virus (variola), include vaccination and drug development. Selective activation of nucleoside analogues by virus-encoded thymidine (dThd) kinases (TK) represents one of the most successful strategies for antiviral chemotherapy as demonstrated for anti-herpes drugs. Vaccinia virus TK is a close orthologue of variola TK but also shares a relatively high sequence identity to human type 2 TK (hTK), thus achieving drug selectivity relative to the host enzyme is challenging.

Results: In order to identify any differences compared to hTK that may be exploitable in drug design, we have determined the crystal structure of VVTK, in complex with thymidine 5'-triphosphate (dTTP). Although most of the active site residues are conserved between hTK and VVTK, we observe a difference in conformation of residues Asp-43 and Arg-45. The equivalent residues in hTK hydrogen bond to dTTP, whereas in subunit D of VVTK, Asp-43 and Arg-45 adopt a different conformation preventing interaction with this nucleotide. Asp-43 and Arg-45 are present in a flexible loop, which is disordered in subunits A, B and C. The observed difference in conformation and flexibility may also explain the ability of VVTK to phosphorylate (South)-methanocarbathymine whereas, in contrast, no substrate activity with hTK is reported for this compound.

Conclusion: The difference in conformation for Asp-43 and Arg-45 could thus be used in drug design to generate VVTK/Variola TK-selective nucleoside analogue substrates and/or inhibitors that have lower affinity for hTK.

Background

Thymidine kinases form part of the salvage pathway for pyrimidine deoxyribonucleotide synthesis. TKs are expressed in a variety of organisms from human to bacteria as well as in a number of viruses. The reaction catalysed by TK involves the transfer of a γ-phosphoryl moiety from ATP to 2'deoxy-thymidine (dThd) to produce thymidine 5'-monophosphate (dTMP). Certain TKs, such as those from herpes simplex virus type 1 (HSV-1) and varicella zoster virus (VZV) have, in addition, thymidylate kinase

activity allowing the conversion of dTMP to thymidine 5'-diphosphate (dTDP). TKs can be classified into two types which differ in several respects [1]. Type 1 TKs are of higher molecular weight, typically around 40 kDa, and are active as homodimers. This subfamily contains the HSV1, HSV2 and VZV TKs, and also mitochondrial TK.

TKs of type 2 include those from poxviridae such as vaccinia virus (VV) and variola virus, [2], as well as from human [3] hTK, (human type II thymidine kinase 1) and mouse [4]. Type 2 TKs have a smaller polypeptide chain compared to type 1, being of ~25 KDa but form homotetramers. They are sensitive to the feedback inhibitors dTDP or dTTP, which are generated at the end of the metabolic pathway [5]. Type 2 TKs have a much narrower substrate specificity compared to type 1 TKs and only phosphorylate 2'deoxyuridine (dU) and/or dThd [6]. For example, the antiherpetic drug (*E*)-5-(2-bromovinyl)-dUrd (BVDU) [7] is not metabolised by the type 2 TKs (i.e. cytosolic TK) in contrast to the type 1 TKs (i.e. mitochondrial TK, HSV-1 TK) which can phosphorylate a variety of (5-substituted) nucleoside analogues including BVDU. Moreover, HSV-1 and HSV-2 TK can even recognize (acyclic) purine nucleoside analogues such as acyclovir and ganciclovir [8]. This difference in substrate specificity is the basis of some selective antiviral drug action as validated by the activation of nucleoside analogues by certain herpes virus TKs. Moreover, herpes TKs are also being studied as suicide genes in a combined gene/chemotherapy strategy to treat cancer [9].

The World Health Organisation declared in 1980 that smallpox had been eradicated. Since then, routine inoculation with the vaccinia virus vaccine was discontinued, resulting in minimal or even non-existent smallpox immunity in the human population [10]. Today, the potential use of smallpox virus as a biological weapon is a major cause for concern, particularly in the context of current low levels of herd immunity to the virus. Additionally, the re-emergence of monkeypox virus infection in humans (mainly in Africa but some cases have also been reported in the United States [11]), has lead to the stockpiling of smallpox vaccine (VV), mainly in developed countries [12]. Nevertheless, some adverse reactions which are sometimes lethal, following vaccination have been reported [13-15]. VV should neither be given to pregnant women for example, nor to people who have a weakened immune system, skin problems like eczema, heart problems or to children under one year old [12]. Thus, specific anti-variola drugs need to be developed as a matter of priority, particularly for widespread use in a bioterrorism emergency, as well as for specific cases of unwanted contamination by VV or complications like eczema vaccinatum or progressive vaccinia. Such drugs would be of particular importance if more virulent strains of variola virus were engineered using genetic modifications. Worryingly, one of the only anti-variola drugs available, cidofovir [16], has been reported to be inefficient against several pox viral strains [17].

Herpes virus TKs have been exploited in the selective activation of nucleoside analogues such as acyclovir, which have spawned a series of highly successful anti-herpetic drugs [18]. The same approach may therefore be applicable in the case of orthopoxviruses. Further understanding of the structural differences between type 1 and 2 TKs would also greatly help to improve and/or create specific drugs against the type 1 TK. Indeed, a drug would be selective if it is preferentially metabolised by the type 1 and not the type 2 TKs or *vice versa*. Thus gathering structural information about both TK types is likely to be of great importance in assisting drug design. So far, HSV1 TK [19,20] and VZV TK [21] structures have been solved, whilst for type 2 TK, the structure of human cytosolic thymidine kinase [22,23] and the TK of *Ureaplasma ureolyticum* recently became available [22,24]. Moreover, determining the structure of different type 2 TKs could help as in the case of orthopox viruses, to design virus TK-specific drugs. Recently, 5-(2-amino-3-cyano-5-oxo-5,6,7,8-tetrahydro-4*H*-chromen-4-yl)-1-(2-deoxy-pentofuranosyl)pyrimidine-2,4-(1*H*,3*H*)-dione has been shown to be phophorylated specifically by vaccinia and cowpox virus TKs [25].

We report here for the first time, the structure of VVTK, one of the smallest type 2 TKs known, in complex with dTTP at 3.1 Å resolution. This work will be of use, in combination with the previous type 2 TK structures, to design or improve type 1 TK-selective drugs as well as drugs that show selectivity against orthopox virus TKs such as VVTK or Variola TK.

Results and discussion

VVTK enzyme kinetics

Assessment of the activity of VVTK to phosphorylate various nucleosides showed its ability to recognize both dCyd and dThd amongst the natural substrates. The efficiency of dCyd phosphorylation was, however, much less (<5%) compared to that with dThd (Fig. 1). In contrast, purified cytosolic TK showed a poor, if any, recognition of dCyd (data not shown). VVTK also efficiently converted the thymidine analogues araT and AZT to their corresponding mono-phosphates whereas no substrate activity was observed for the purine nucleosides araA, dA, dG and CdA. In this respect, VVTK behaves more similarly to cytosolic TK (Fig. 1). Also, dTTP inhibits the phosphorylation of dThd (1 μM) by VVTK with an IC_{50} (50% inhibitory concentration) of 14 ± 4.0 μM, whereas the corresponding IC_{50} for cytosolic TK was markedly lower (2.8 ± 0.5 μM).

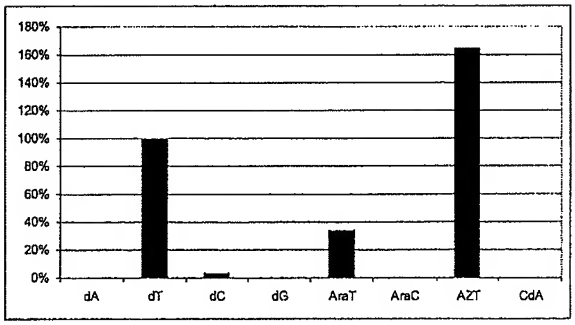

Figure 1
Histogram showing substrate activity of certain nucleosides with VVTK.

Overall structure of VVTK

The quaternary structure of VVTK (Fig. 2a and 2b) is tetrameric. which is similar to that of hTK [22,23]. hTK shares 66% amino acid sequence identity with VVTK, showing a conserved fold amongst species (Fig. 2b). The four VVTK subunits within the tetramer are identical apart from a flexible loop (residues 40 to 60) situated on the surface. In the other type 2 TK structures [22-24], the equivalent loop is either not visible or appears to be in a different conformation from one monomer to the other, indicating that this flexibility is common to Type 2 TKs. It has been inferred that this loop might be involved in phosphoryl donor interaction [24].

As found in other type 2 TKs, VVTK has a central α/β domain structure consisting of six parallel β-strands surrounded by helices (Fig. 2a). Above the α/β domain, a zinc-binding domain is present, the latter belongs to the structural zinc-binding class [26]. Although no zinc was added during purification or crystallization, the metal is present in the structure and coordinated to four cysteines. This metal is believed to play a structural role, stabilising the adjacent loop, or lasso domain, involved in nucleoside binding via residues Tyr-166 and Arg-150. The cysteines involved in zinc binding are also found in the hTK, whilst in the case of the *Ureaplasma* enzyme, the last cysteine is substituted by a histidine [22].

Active site structure of VVTK

VVTK crystals grew in the presence of dTTP, the feedback inhibitor of the pathway. The binding of dTTP in VVTK is similar to that observed in the hTK structure. The phosphates of dTTP bind to the α/β domain, whereas the thymine base and the deoxyribose bind between the lasso domain and the α/β domain (Figs. 2a, 3c). The thymine moiety is bound to the backbone of the protein via residues Phe-113, Ile-157 and 159. Thus this region of the enzyme appears unsuitable for use in designing species-selective ligands as no side-chain contacts are present (Fig. 2c).

Whilst most of the VVTK active site residues are conserved and superimpose well with the human TK, nevertheless, some significant differences are apparent. In the VVTK active site Ser-148 replaces the equivalent residue in hTK, Thr-163, a serine being also present in UuTK. Welin *et al*, proposed that this position, relatively close to the 5-methyl group of dTTP, could be used in the design of selective nucleoside analogues for UuTK versus the human enzyme. Indeed the pocket around the 5-methyl group of dTTP is slightly larger compared to the pocket of hTK, so substitutions at the 5 position of dThd could be explored [24]. Based on the same argument, these kinds of analogues may also be effective with VVTK and UuTK but not hTK.

A further important difference in the VVTK active site is the conformation of Asp-43 and Arg-45 (Fig. 3b). The equivalent residues in hTK are in close contact with the 3'-oxygen of the deoxyribose and to the β-phosphoryl oxygen of dTTP respectively, whereas they are not in the case of VVTK. Asp-43 and Arg-45 are only observed in the VVTK subunit D, they are disordered in the other three subunits, indicating the flexible nature of this loop. Nevertheless, the dTTP still adopts the same conformation in each subunit as observed in the human enzyme. We thus can infer that Asp-43 and Arg-45 may not be crucial for the binding of dTTP, otherwise this ligand would either not stay bound to the active site or would shift position. It has been proposed that Arg-60 in hTK (Arg-45 in VVTK) may act to stabilize the transition state of the reaction [22]. From the VVTK structure, it appears that the conformation of this residue has to change to allow contact with the substrate and hence the reaction to occur. The flexibility of this loop region also implies that more space is available in the VVTK active site compared to hTK. Clearly, using bulkier groups at the 3- and 5-positions in the pyrimidine ring of the dThd molecule should be investigated for the rational design of novel, specific drugs against VVTK. Modifying the sugar moiety would also be a worthwhile approach to pursue in the design of further analogues.

Ligand specificity of VVTK

Thymidine analogues such as (South)-methanocarbathymine ((S)-MCT) and (North)-methanocarbathymine ((N)-MCT) (Fig. 4) have been studied as antiviral agents against orthopox and herpes viruses. For orthopox viruses, such as variola and vaccinia viruses, ((N)-MCT has potent antiviral activity whilst ((S)-MCT) does not [27,28]. Due

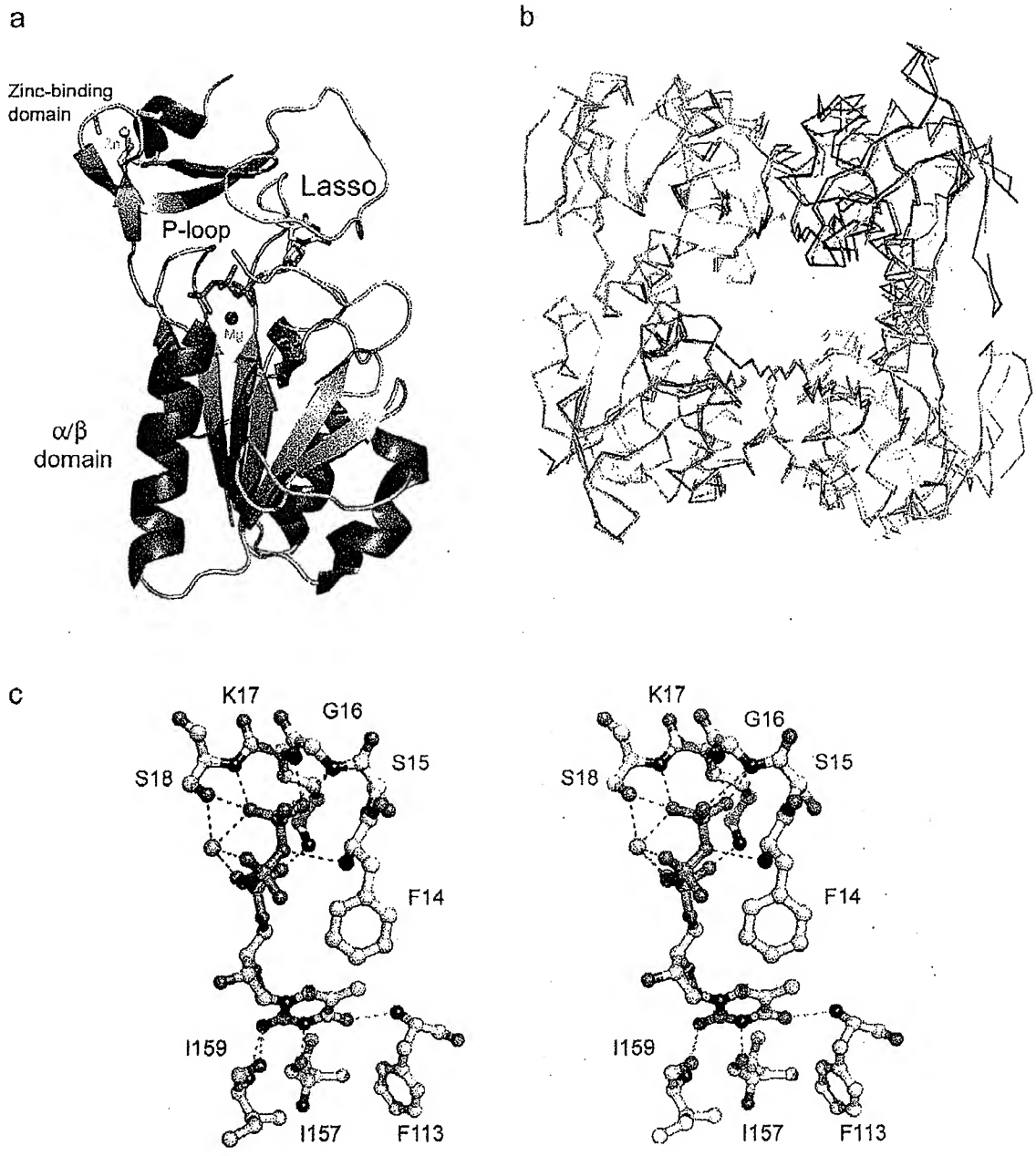

Figure 2

a. Diagram showing one VVTK monomer complexed with dTTP and magnesium. α-helices are shown in red/grey, β-strands are in blue/grey with loops in gold. dTTP is in standard atom colors and the magnesium ion is in blue. **b.** Diagram showing the superimposition of α-carbons of hTK (grey) and VVTK. Each VVTK subunit is shown in different colors (green/red/yellow/blue). **c.** Stereo-diagram of the VVTK active site showing residues that interact with dTTP and magnesium. Protein side-chains and main-chain carbon atoms are in grey, main-chain N and O atoms are in blue and red respectively). dTTP is drawn in standard atom colors with the magnesium ion in green

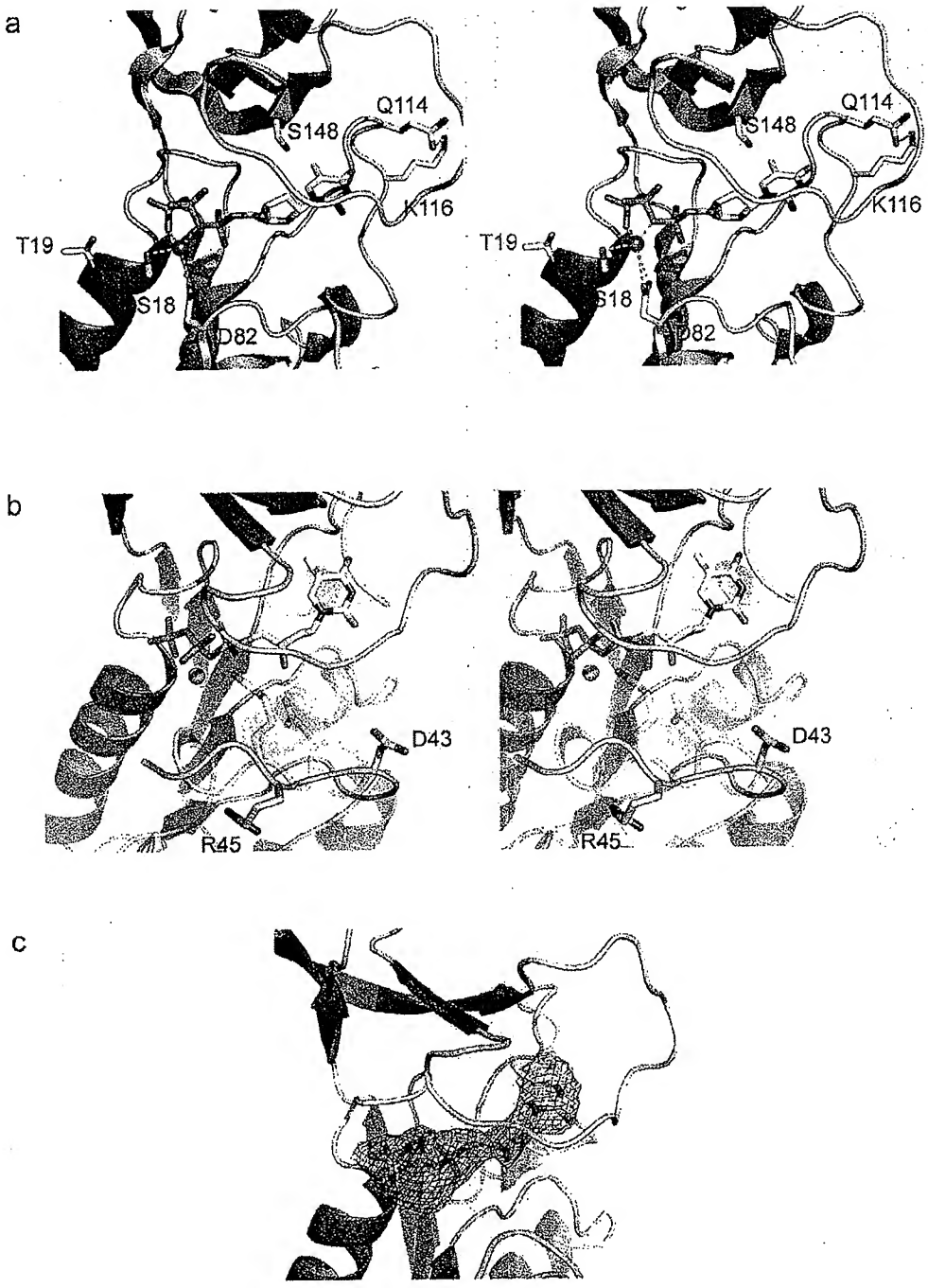

Figure 3
a. Stereo-diagram highlighting the positions ofresidues studied in site-directed mutagenesis experiments of VVTK. Side chains subjected to mutation are shown in grey. **b.** Stereo-diagram showing the different conformations of residues Asp-43 and Arg-45 in subunit D of VVTK and the equivalent hTK residues colored in cyan. **c.** Diagram showing the final 2fo-fc map contored at 1σ for dTTP and magnesium. Color coding for the protein secondary structure is as for Fig 2a.

to the pseudo-ring conformation, ((S)-MCT) has been reported to be the preferred substrate of herpes TKs, whereas ((N)-MCT) is preferred by the cellular DNA polymerases [29]. Prichard *et al* suggested that ((N)-MCT) could also be phosphorylated by type 2 TKs from cowpox and vaccinia viruses [28], whereas Smee *et al* inferred that orthopoxvirus TKs are not responsible for the formation of phosphorylated ((N)-MCT) [27]. It has also been shown that hTK has a weak affinity for ((N)-MCT) and essentially no affinity for ((S)-MCT) [29]. ((S)-MCT) inhibits growth of HSV1 TK transduced osteosarcoma cells [30], thus hTK alone could not be involved in drug activation. The MCT activity seems to be highly dependent on the particular cell line, which is thus a consideration in validating a particular result. Thus the test system ultimately of most relevance to human therapy would involve primates [27].

Nevertheless, HPLC activity assays have shown that ((S)-MCT) can be phosphorylated by VVTK [23], thus MCT modeled in the VVTK active site structure could be used as a basis for drug design. The superimposition of (S)-MCT and dTTP shows that the thymine ring and the sugar/pseudo-sugar match very well. As the (S)-MCT can be phosphorylated, this suggests that the conformation of the dThd moiety of dTTP has a very similar conformation to the dThd substrate in VVTK. This has been confirmed by the recent structure of UuTK complexed with dThd (PDB code: 2B8T) [24]. The fact that VVTK is able to phosphorylate (S)-MCT suggests that a larger sugar moiety can fit into the active site. Such a difference in substrate specificity between hTK and VVTK might be due to the flexibility of the loop containing Arg-45 (Arg-60 in hTK).

Further suggestion that the plasticity of the VVTK active site relative to hTK is indicated by the selective phosphorylatioin by VVTK compared to hTK of the bulky molecule 5-(2-amino-3-cyano-5-oxo-5,6,7,8-tetrahydro-4*H*-chromen-4-yl)-1-(2-deoxy-pentofuranosyl)pyrimidine-2,4-(1*H*,3*H*)-dione. The latter drug showed a minimal toxicity to uninfected cells and inhibited the replication of vaccinia and cowpox virus [25]. Fan *et al*, suggested that orthopoxvirus kinases are more promiscuous than previously believed. Indeed their substrate specificity seems broader than cellular kinases, thus these enzymes could be exploited in a similar manner to the herpes TKs.

Relating VVTK mutagenesis and structural studies

Prior to the determination of any crystal structure of a type 2 TK, some mutational studies had been reported on VVTK. It has been shown that residue Asp-82 participates in the binding of magnesium [31] (Fig. 3a) and that the loss of a negatively charged residue at this position alters the ability of VVTK to transfer the γ-phosphate moiety of ATP to dThd. It was suggested that Asp-82 is not involved in ATP binding but rather aids its correct orientation for nucleophilic attack. In the VVTK structure, Asp-82 is indeed orientated towards the metal ion and its distance from the magnesium ion varies from one subunit to another (from 3.2 to 3.7 Å).

VVTK mutants Ser18Thr and Thr19Ser (Fig. 3a) [32] have also been studied, and showed an increased activity of 3.7-fold and 1.4-fold, respectively. The equivalent to Thr-19 is conserved in most type 2 TKs although not in the case of *Ureaplasma*, where it is substituted by an alanine and thus is unlikely to be essential for catalysis. Indeed, VVTK mutated in this position to the bulkier residues Asn

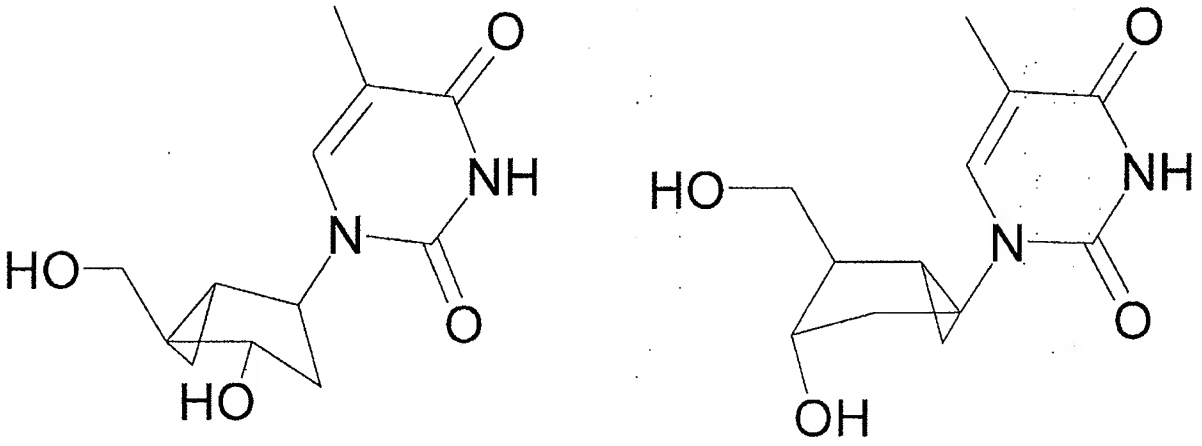

Figure 4
Structure of (north)-methanocarbathymine (left) and (south)-methanocarbathymine (right).

or Arg retains significant activity (~27% of wild-type). Even a Pro-19 mutant retains 10% of wild-type VVTK activity. Thr-19 is not directly involved in dTTP binding but may have a role in ATP binding. As yet no type 2 TK has been solved with bound ATP, hence it is difficult to assess the importance of this residue. The Ser18Thr mutant shows a greater enhancement of enzyme activity (~3.8-fold) than does Thr19Ser and indeed in our structure, Ser-18 forms hydrogen bonds via its main-chain nitrogen to a γ-phosphate oxygen and via its side-chain oxygen to the magnesium and a γ-phosphate oxygen. Thus Ser-18 would appear more crucial for enzyme catalysis than Thr-19. Although Ser-18 is conserved in the hTK structure (Ser-33) it is conservatively substituted for threonine in UuTK (Thr26). The methyl group of the Thr-26 side-chain is in van der Waals contact with Ile-30 (3.8 Å). It is thus possible that replacing the serine by threonine could stabilize the side-chain oxygen in a preferential conformation for substrate binding, which may explain the increased activity of the Ser18Thr mutant VVTK.

Finally, mutational studies have been reported on Gln-114 [33] (Fig. 3a). The authors inferred that Gln-114 participates in the feedback inhibition by dTTP since this mutant TK could bind dTTP yet feedback inhibition was abolished. Interestingly, Gln-114 is not in contact with dTTP, and more surprisingly, it is located on the surface of the tetramer. The effect of mutating Gln-114 to either His or Asp would only be to break the hydrogen bond with the adjacent Lys. In this case, the abolition of the feedback inhibition could only be explained by a destabilization of the loop which is in close contact with the dTTP molecule. However, the mutation does not apparently affect the VVTK activity under standard conditions, thus either the binding of substrates dThd and ATP are not disrupted by this mutation, or if they are, the decrease in apparent affinity is compensated for as a result of an increase in catalytic rate. To clarify this, further experiments would be needed to determine the k_{cat} and K_m of each mutant.

Conclusion

In conclusion, the work reported here provides the first structure of VVTK. Even though showing similarity to the other type 2 TK structures, the detailed comparison of the active site points to principles for designing specific inhibitors of VVTK relative to hTK, mainly by using the fact that the deoxyribose appears able to accept bulkier/modified substituents. This result is consistent with Birringer *et al*'s report of (S)-MCT being phosphorylated by VVTK whilst not being a substrate for hTK [23]. Knowledge of the residues involved in ligand binding of type 2 TKs by structure comparison, might also assist in the design of specific drugs against type 1 TKs.

Methods

Protein purification

The pET-16b-VVTK (derived from Novagen pET-16b) expression plasmid coding for an N-terminal His_6-tagged-VVTK was transformed into Rosetta(DE3)pLysS for protein expression. The cells were grown in a 40 ml Luria Broth starter culture supplemented with 50 μg/ml carbenicillin and 34 μg/ml chloramphenicol, overnight, with shaking at 37°C. The culture was then diluted 1/100 into 4 l of LB and grown at 37°C until the A_{600} reached 0.7. isopropyl-beta-D-thiogalactopyranoside was added to 1 mM and the induction was carried out for 3 hours at the same temperature. The cells were harvested by centrifugation and the pellets were resuspended in buffer A (50 mM sodium inorganic phosphate pH 7.8, 300 mM NaCl). The cells were disrupted by sonication and the supernatant, following clarification by centrifugation, was applied to a 5 ml nickel chelating column (Hi-trap chelating Column, GE Healthcare) pre-equilibrated with buffer A. VVTK was eluted with buffer A + 500 mM imidazole. Fractions containing VVTK were applied to a Superdex S200 16/60 gel filtration column pre-equilibrated with 50 mM Tris-HCl pH 7.8 and 200 mM NaCl. The fractions containing VVTK were pooled and buffer exchanged against 20 mM Tris-HCl pH 8 and finally, concentrated to 22 mg/ml. The purification protocol produced on average 25 mg of VVTK per litre of culture.

Crystallisation and data collection

Thymidine triphosphate, dithiothreitol and $MgCl_2$ were added to VVTK for initial screening in several Hampton, Wizard and Emerald kits in a total of 768 conditions. A Cartesian Technologies pipetting robot was used to set up 100 + 100 nl sitting drops in Greiner 96-well plates which were placed in a TAP storage vault [19]. After optimisation, crystals grew in 2–7% polyethylene glycol 3350, 5 mM $MgSO_4$ and 50 mM MES pH6.5. Even though the crystals were small (50 μm in the longest dimension), they were suitable for data collection.

X-ray diffraction data were collected at 100 K in-house using a Rigaku MicroMax 007 generator Cu Kα radiation source and a MAR 345 imaging plate detector (MAR Research). Crystals diffracted to a resolution limit of 3.1 Å. Images were indexed and integrated with DENZO, whilst data were merged using SCALEPACK [34]. The crystals belong to space group $P3_1$ with unit cell lengths of $a = b = 63.3$, $c = 166.4$ (Å), and contained four VVTK subunits within the asymmetric unit. Detailed statistics for X-ray data collection are given in Table 1.

The VVTK crystal structure was solved by molecular replacement using MOLREP [35] with the coordinates of hTK (PDB code 1W4R) [23] as the search model. Refinement was carried out using cycles of manual rebuilding

Table 1: Statistics for crystallographic structure determination

Data collection details:	
Data collection site	In house
Detector	MAR345
Wavelength (Å)	1.5418
Resolution range (Å)	30.0-3.1 (3.21-3.10)
Number of unique reflections	13636
Redundancy	3.8 (2.8)
Completeness (%)	94.8 (87.9)
Average $I/\sigma(I)$	8.5 (2.3)
Rmerge[a]	0.149 (0.494)
Refinement statistics:	
Resolution range (Å)	30.0-3.1 (3.18-3.1)
R-factor†(R_{work}/R_{free})[b]	25.7/28.9
Number of protein atoms	5206
Average B factor (Å^2)	42.3
Rms bond length deviation (Å)	0.012
Rms bond angle deviation (°)	1.42

Figures in brackets – outer shell data. [a]$R_{merge} = \Sigma|I - \langle I\rangle|/\Sigma\langle I\rangle$; [b]R factor = $\Sigma|F_o - F_c|/\Sigma F_o$.

with COOT [36], followed by NCS restrained refinement using CNS [37] and REFMAC5 [38] with TLS [39]. Real space electron density averaging applied to the four molecules in the VVTK crystal asymmetric unit was carried out using the program GAP (D. I. Stuart, J. M. Grimes & J. M. Diprose, unpublished). Density for the dTTP ligand was fitted as appropriate and refined. The final refinement parameters of R_{work} and R_{free} were 25.7 and 28.9% respectively (Table 1). Structural superpositions were performed with SHP [40], and figures were drawn using PYMOL (DeLano, W.L. (2002) DeLano Scientific, San Carlos, CA, USA). The coordinates of VVTK together with structure factors have been deposited in the protein data bank (PDB code 2J87).

Enzyme assays

Thymidine kinase assays were carried out in a 50 µl reaction mixture containing : 50 mM Tris_HCl pH7.6, 0.1 mg/ml BSA, 2.5 mM γ-^{32}[P] ATP, 5 mM $MgCl_2$, 5 mM dithiothreitol, and nucleoside analogs. In the assays with dThd, 2'-deoxycytidine, 2'-deoxyadenine and 2'-deoxyguanosine, 1 mM of nucleoside analog was used, in the other assays, 150 µM of nucleoside was used. The samples were incubated for 30 min at 37°C. The substrate specificity of the purified enzyme was assayed by thin layer chromatography. The autoradiography was scanned with a "Biorad Personal Molecular Image FX" and the was interpreted with "Quantity one" software also from Biorad.

Abbreviations

TK, thymidine kinase; VVTK, vaccinia virus thymidine kinase; hTK, human type II thymidine kinase 1; UuTK, *Ureaplasma urealyticum* thymidine kinase; dThd, 2'-deoxythymidine; dTTP, thymidine 5'-triphosphate; dTD(M)P, thymidine 5'-di(mono)phosphate; (S)-MCT, (South)-methanocarbathymine; (N)-MCT, (North)-methanocarbathymine.

Authors' contributions

KEO purified, crystallized the protein; collected and processed the diffraction data, modelled, refined and analyzed the structure. NS cloned the gene. JB carried out enzymatic studies. DKS, JB, AK coordinated the study. KEO and DKS prepared the manuscript with additional input from JB and AK. All authors read and approved the final manuscript.

Acknowledgements

We thank the EC for funding this work via project QLRT-2000-01004. Additional support was from the UK Medical Research Council, the K.U. Leuven (G.O.A 2005/19) and FWO (G-0267-04) and by grants from the Swedish Cancer Society and the Swedish Research Council (AK) We thank Robert Esnouf and Jun Dong for computer support.

References

1. Black ME, Hruby DE: **Quaternary structure of vaccinia virus thymidine kinase.** *Biochem Biophys Res Commun* 1990, **169(3):**1080-1086.
2. Esposito JJ, Knight JC: **Nucleotide sequence of the thymidine kinase gene region of monkeypox and variola viruses.** *Virology* 1984, **135(2):**561-567.
3. Flemington E, Bradshaw HDJ, Traina-Dorge V, Slagel V, Deininger PL: **Sequence, structure and promoter characterization of the human thymidine kinase gene.** *Gene* 1987, **52(2-3):**267-277.
4. Lin PF, Lieberman HB, Yeh DB, Xu T, Zhao SY, Ruddle FH: **Molecular cloning and structural analysis of murine thymidine kinase genomic and cDNA sequences.** *Mol Cell Biol* 1985, **5(11):**3149-3156.
5. Hruby DE: **Inhibition of vaccinia virus thymidine kinase by the distal products of its own metabolic pathway.** *Virus Res* 1985, **2(2):**151-156.
6. Arner ES, Eriksson S: **Mammalian deoxyribonucleoside kinases.** *Pharmacol Ther* 1995, **67(2):**155-186.
7. De Clercq E: **Discovery and development of BVDU (brivudin) as a therapeutic for the treatment of herpes zoster.** *Biochem Pharmacol* 2004, **68(12):**2301-2315.
8. Vogt J, Perozzo R, Pautsch A, Prota A, Schelling P, Pilger B, Folkers G, Scapozza L, Schulz GE: **Nucleoside binding site of herpes simplex type 1 thymidine kinase analyzed by X-ray crystallography.** *Proteins* 2000, **41(4):**545-553.
9. Kohn DB, Sadelain M, Dunbar C, Bodine D, Kiem HP, Candotti F, Tisdale J, Riviere I, Blau CA, Richard RE, Sorrentino B, Nolta J, Malech H, Brenner M, Cornetta K, Cavagnaro J, High K, Glorioso J: **American Society of Gene Therapy (ASGT) ad hoc subcommittee on retroviral-mediated gene transfer to hematopoietic stem cells.** *Mol Ther* 2003, **8(2):**180-187.
10. Breman JG, Arita I: **The confirmation and maintenance of smallpox eradication.** *N Engl J Med* 1980, **303(22):**1263-1273.
11. Reed KD, Melski JW, Graham MB, Regnery RL, Sotir MJ, Wegner MV, Kazmierczak JJ, Stratman EJ, Li Y, Fairley JA, Swain GR, Olson VA, Sargent EK, Kehl SC, Frace MA, Kline R, Foldy SL, Davis JP, Damon IK: **The detection of monkeypox in humans in the Western Hemisphere.** *N Engl J Med* 2004, **350(4):**342-350.
12. Moore ZS, Seward JF, Lane JM: **Smallpox.** *Lancet* 2006, **367(9508):**425-435.
13. Ratner LH, Lane JM, Vicens CN: **Complications of smallpox vaccination: surveillance during an island-wide program in Puerto Rico, 1967-1968.** *Am J Epidemiol* 1970, **91(3):**278-285.
14. Mellin H, Neff JM, Garber H, Lane JM: **Complications of smallpox vaccination, Maryland. 1968.** *Johns Hopkins Med J* 1970, **126(3):**160-168.

15. Lane JM, Ruben FL, Abrutyn E, Millar JD: **Deaths attributable to smallpox vaccination, 1959 to 1966, and 1968.** *Jama* 1970, **212(3):**441-444.
16. De Clercq E: **Acyclic nucleoside phosphonates in the chemotherapy of DNA virus and retrovirus infections.** *Intervirology* 1997, **40(5-6):**295-303.
17. Smee DF, Sidwell RW, Kefauver D, Bray M, Huggins JW: **Characterization of wild-type and cidofovir-resistant strains of camelpox, cowpox, monkeypox, and vaccinia viruses.** *Antimicrob Agents Chemother* 2002, **46(5):**1329-1335.
18. Naesens L, De Clercq E: **Recent developments in herpesvirus therapy.** *Herpes* 2001, **8(1):**12-16.
19. Walter TS, Diprose JM, Mayo CJ, Siebold C, Pickford MG, Carter L, Sutton GC, Berrow NS, Brown J, Berry IM, Stewart-Jones GB, Grimes JM, Stammers DK, Esnouf RM, Jones EY, Owens RJ, Stuart DI, Harlos K: **A procedure for setting up high-throughput nanolitre crystallization experiments. Crystallization workflow for initial screening, automated storage, imaging and optimization.** *Acta Crystallogr D Biol Crystallogr* 2005, **61(Pt 6):**651-657.
20. Wild K, Bohner T, Folkers G, Schulz GE: **The structures of thymidine kinase from herpes simplex virus type 1 in complex with substrates and a substrate analogue.** *Protein Sci* 1997, **6(10):**2097-2106.
21. Bird LE, Ren J, Wright A, Leslie KD, Degreve B, Balzarini J, Stammers DK: **Crystal structure of varicella zoster virus thymidine kinase.** *J Biol Chem* 2003, **278(27):**24680-24687.
22. Welin M, Kosinska U, Mikkelsen NE, Carnrot C, Zhu C, Wang L, Eriksson S, Munch-Petersen B, Eklund H: **Structures of thymidine kinase 1 of human and mycoplasmic origin.** *Proc Natl Acad Sci U S A* 2004, **101(52):**17970-17975.
23. Birringer MS, Claus MT, Folkers G, Kloer DP, Schulz GE, Scapozza L: **Structure of a type II thymidine kinase with bound dTTP.** *FEBS Lett* 2005, **579(6):**1376-1382.
24. Kosinska U, Carnrot C, Eriksson S, Wang L, Eklund H: **Structure of the substrate complex of thymidine kinase from Ureaplasma urealyticum and investigations of possible drug targets for the enzyme.** *Febs J* 2005, **272(24):**6365-6372.
25. Fan X, Zhang X, Zhou L, Keith KA, Prichard MN, Kern ER, Torrence PF: **Towards orthopoxvirus coutermeasures: a novel heteromorphic nucleoside of unusual structure.** *J Med Chem* 2006, **49(14):**4052-4054.
26. Vallee BL, Auld DS: **Functional zinc-binding motifs in enzymes and DNA-binding proteins.** *Faraday Discuss* 1992:47-65.
27. Smee DF, Wandersee MK, Bailey KW, Wong MH, Chu CK, Gadthula S, Sidwell RW: **Cell line dependency for antiviral activity and in vivo efficacy of N-methanocarbathymidine against orthopoxvirus infections in mice.** *Antiviral Res* 2006.
28. Prichard MN, Keith KA, Quenelle DC, Kern ER: **Activity and mechanism of action of N-methanocarbathymidine against herpesvirus and orthopoxvirus infections.** *Antimicrob Agents Chemother* 2006, **50(4):**1336-1341.
29. Marquez VE, Ben-Kasus T, Barchi JJJ, Green KM, Nicklaus MC, Agbaria R: **Experimental and structural evidence that herpes 1 kinase and cellular DNA polymerase(s) discriminate on the basis of sugar pucker.** *J Am Chem Soc* 2004, **126(2):**543-549.
30. Schelling P, Claus MT, Johner R, Marquez VE, Schulz GE, Scapozza L: **Biochemical and structural characterization of (South)-methanocarbathymidine that specifically inhibits growth of herpes simplex virus type 1 thymidine kinase-transduced osteosarcoma cells.** *J Biol Chem* 2004, **279(31):**32832-32838.
31. Black ME, Hruby DE: **Site-directed mutagenesis of a conserved domain in vaccinia virus thymidine kinase. Evidence for a potential role in magnesium binding.** *J Biol Chem* 1992, **267(10):**6801-6806.
32. Black ME, Hruby DE: **Identification of the ATP-binding domain of vaccinia virus thymidine kinase.** *J Biol Chem* 1990, **265(29):**17584-17592.
33. Black ME, Hruby DE: **A single amino acid substitution abolishes feedback inhibition of vaccinia virus thymidine kinase.** *J Biol Chem* 1992, **267(14):**9743-9748.
34. Otwinowski Z, Minor W: **Processing of X-ray diffraction data collected in oscillation mode.** *Methods Enzymol* 1996, **276:**307-326.
35. Vagin A, Teplyakov A: **MOLREP: an automated program for molecular replacement.** *J Appl Cryst* 1997, **30:**1022-1025.
36. Emsley P, Cowtan K: **Coot: model-building tools for molecular graphics.** *Acta Crystallogr D Biol Crystallogr* 2004, **60(Pt 12 Pt 1):**2126-2132.
37. Brunger AT, Adams PD, Clore GM, DeLano WL, Gros P, Grosse-Kunstleve RW, Jiang JS, Kuszewski J, Nilges M, Pannu NS, Read RJ, Rice LM, Simonson T, Warren GL: **Crystallography & NMR system: A new software suite for macromolecular structure determination.** *Acta Crystallogr D Biol Crystallogr* 1998, **54(Pt 5):**905-921.
38. Murshudov GN, Vagin AA, Dodson EJ: **Refinement of macromolecular structures by the maximum-likelihood method.** *Acta Crystallogr D Biol Crystallogr* 1997, **53(Pt 3):**240-255.
39. Winn MD, Isupov MN, Murshudov GN: **Use of TLS parameters to model anisotropic displacements in macromolecular refinement.** *Acta Crystallogr D Biol Crystallogr* 2001, **57(Pt 1):**122-133.
40. Stuart DI, Levine M, Muirhead H, Stammers DK: **Crystal structure of cat muscle pyruvate kinase at a resolution of 2.6 A.** *J Mol Biol* 1979, **134(1):**109-142.

Exhibit C

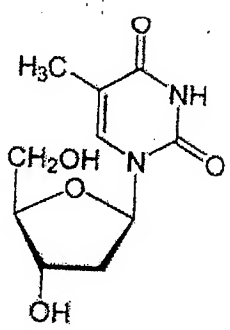

+ ATP --->

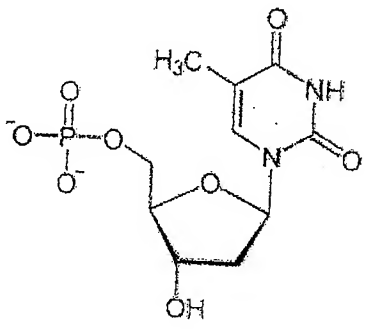

+ ADP

Exhibit D

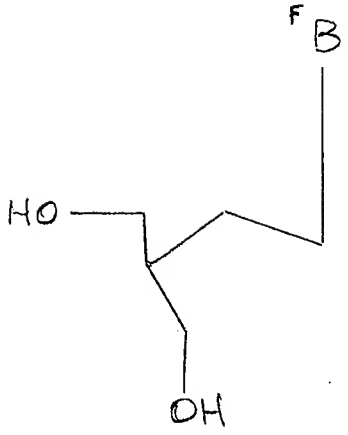

FPCV

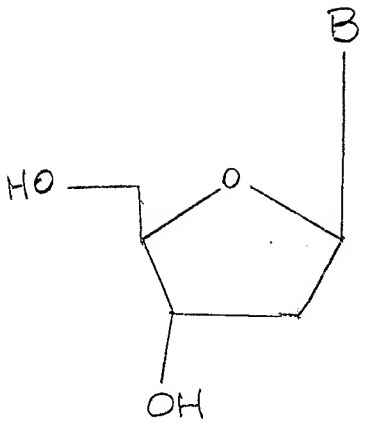

Thymidine

Exhibit E

Understanding the Binding of 5-Substituted 2′-Deoxyuridine Substrates to Thymidine Kinase of Herpes Simplex Virus Type-1

Hans De Winter and Piet Herdewijn*

Laboratory of Medicinal Chemistry, Rega Institute for Medical Research, Katholieke Universiteit Leuven, Minderbroedersstraat 10, B-3000 Leuven, Belgium

Received April 10, 1996

Thymidine kinase from HSV-1 (HSV-1 TK) is a key enzyme in the metabolic activation of antiviral nucleosides. High affinity of such compounds for the enzyme is required for efficient phosphorylation. In this study, affinity data from a series of 5-substituted 2′-deoxyuridine substrates in combination with the crystal structure of the viral enzyme were used to investigate the structural factors influencing the affinity of these compounds for the enzyme. Calculations showed that the binding energetics and conformations of thymidine and the 5-substituted 2′-uridine analogues are similar. The major part of the binding energy arises from interactions involving sugar and base moieties. Small differences in affinity for the enzyme are explained by the hydrophobicity of the 5-substituent or by its energetic complementarity with the active site pocket. In designing high-affinity nucleoside substrates of HSV-1 TK, care should be taken to maintain the geometry of the base moiety and sugar hydroxyl functionalities. Substitutions at the 5 position of the nucleobase should be lipophilic and characterized by well-defined geometrical properties. The present study represents a first quantitative explanation for HSV-1 TK affinity of 5 substituted 2′ deoxyuridines which are historically the first group of selective antivirals. The results may be used to design new and more potent compounds.

Introduction

Herpes simplex virus (HSV) establishes latent infections in human nerve tissue and exists as type-1 (HSV-1) and type 2 (HSV-2). Infections of HSV-1 in humans can lead to acute gingivostomatitis, herpes labialis, or ocular disease, while HSV-2 accounts for most cases of herpes genitalis.

Antiviral chemotherapy started with the discovery in 1959 of the antiherpes activity of 5-iodo-2′-deoxyuridine by serendipity.[1] The structure of 5-iodo-2′-deoxyuridine is very similar to that of thymidine, *i.e.* the replacement of the methyl group in the 5-position of the uracil moiety by a iodine. This small difference, however, is sufficient to render 5-iodo-2′-deoxyuridine a selective antiviral compound. This landmark in antiviral chemotherapy was later followed by others; the most important are the discovery of acyclovir as a nontoxic antiherpes agent and the discovery of 3′-azido-3′-deoxythymidine as the first approved anti-HIV nucleoside. The resemblance of this latter molecule with the structure of thymidine is also striking. Here the 3-hydroxyl group of the deoxyribose moiety is replaced by an azido group. Both compounds (5-iodo-2′-deoxyuridine and 3′-azido-3′-deoxythymidine) also demonstrate a very similar mode of action. They have to be phosphorylated to their corresponding triphosphate, and in this form they selectively interact with viral enzymes (DNA polymerase and reverse transcriptase, respectively). Although the structure of 5-iodo-2′-deoxyuridine and its mode of action have been known for over 30 years, the way it interacts with its metabolic and target enzymes still remains puzzling.

The discovery of 5-iodo-2′-deoxyuridine as a selective HSV-1 drug has led to the synthesis of an overwhelming number of other 5-substituted 2′-deoxyuridine compounds (for a review, see ref 2), of which the best known is (*E*)-5-(bromovinyl)-2′-deoxyuridine.[3] Structure–activity studies of this class of compounds have only been descriptive until now after the recent discovery of a new series of 5-heteroaromatic-substituted 2′-deoxyuridines and the availability of the crystal structure of herpes simplex type 1 thymidine kinase.

The genome of HSV-1 encodes several virus specific enzymes involved in nucleoside metabolism, one of them being thymidine kinase (TK). This enzyme phosphorylates thymidine to its corresponding 5′-monophosphate, using ATP as its phosphoryl source. Therefore, TK is a crucial enzyme in the salvage pathway of thymidine-5′-triphosphate, which is the precursor of the thymidine incorporated in DNA. Viral TKs differ in many aspects from human TK and are therefore important targets for chemotherapy. The viral enzymes have much broader substrate specificity than the corresponding human enzyme, which only recognizes thymidine as a substrate while the viral enzymes even accept L-thymidine, guanine nucleosides, carbocyclic nucleosides, and many 5-substituted 2′-deoxyuridine analogues.[4]

HSV-1 TK is not essential for viral replication in cell culture, but it is an important enzyme for the pathogenicity of the virus.[5,6] However, also significant for the design of antiviral compounds is that HSV-1 TK is a key enzyme in the metabolic activation of modified nucleosides as antiviral agents. The general mode of action of these types of antiviral agents is that they are phosphorylated to their 5′-monophosphates by HSV-1 TK. The modified nucleosides have a much higher affinity for HSV-1 TK than for the cellular enzyme, and therefore preferential phosphorylation occurs mainly in virus-infected cells. The 5′-monophosphates are then further phosphorylated to their 5′-triphosphates by several other cellular kinases, and these triphosphates can either act as competitive inhibitors to TTP of the viral DNA polymerase or function as substrates for this enzyme and become incorporated into the viral DNA.

* Abstract published in *Advance ACS Abstracts* October 15, 1996.

S0022-2623(96)00278-6 CCC: $12.00

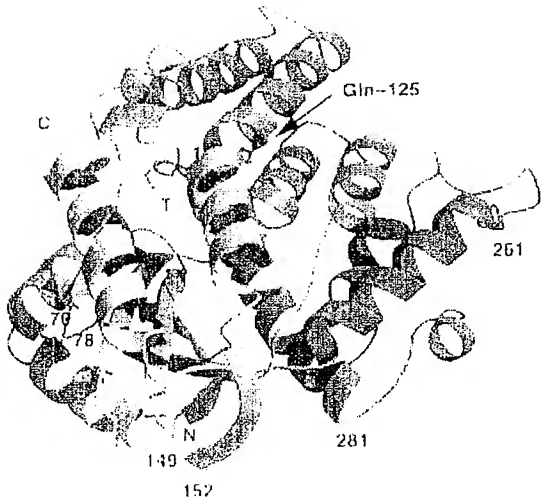

Figure 1. An outline of HSV-1 thymidine kinase. Thymidine (T) and Gln 125 emphasize the location of the active site pocket. Loops between residues 149–152, 70–78, and 261–281 are missing from the crystal structure. The C- and N-termini are labeled C and N, respectively.

Thymidine kinase, whose crystal structure has recently been solved at 2.8 and 2.2 Å resolution for the complexes with thymidine and ganciclovir, respectively,[7] is the first enzyme involved in the metabolic activation of antiviral nucleosides. Therefore, it might be advantageous for an effective anti-HSV-1 nucleoside to show high affinity for the viral thymidine kinase. Thus, any project which targets the design of modified nucleosides as anti-HSV compounds should incorporate some estimates on the rate of phosphorylation of the designed nucleosides by viral TK, and hence should develop an understanding about the interaction of HSV-1 TK with its substrates at the molecular level.

In the present work, computer simulations were used to investigate these interactions and to examine structural features important for 5-substituted 2′-deoxyuridine substrate recognition by HSV-1 TK. This series of 5-substituted nucleosides, recently discovered by our group, are selectively phosphorylated by HSV-1 TK.[8-10] Their affinity for the enzyme, expressed in terms of IC_{50} values measured against the natural substrate, ranges from 2 to 150 μM, depending on the substitution pattern at the 5 position. These compounds differ from the natural substrate thymidine only by a different substitution at the 5 position and provide, therefore, an interesting tool for the analysis of the nature of molecular recognition between HSV-1 TK and 5-substituted 2′-deoxyuridine analogues. It is expected that the results of this study may be of potential interest to drug designers and chemists in their search for improved HSV-1 antivirals. Moreover, this study gives a theoretical basis for an historical discovery in antiviral chemotherapy.

The Players

The Crystal Structure of HSV-1 TK. HSV-1 TK has been crystallized in complex with either thymidine or ganciclovir.[7] The molecule consists of an ab structure made up of 13 α-helices, two 3_{10}-helices, and seven β-sheets (Figure 1). The five stranded β-sheet forms part of the core of the molecule, which contains the active site. Although the sugar equivalents of both ligands exhibit similar binding arrangements in the active-site pocket, comparison of the nucleobase of ganciclovir with that of thymidine shows that the guanine base is flipped by approximately 180°, so that its O6 atom is located in a pocket on the opposite side of the 5-methyl group of thymidine (Figure 2). As a result of these different binding modes, and because of the high structural resemblance between thymidine and the substrates used for this study, we have taken the crystal structure of the thymidine–TK complex as the starting point for all modeling experiments. It should be noted that, apart from the amide function of Gln 125 which is rotated by 180°, no other remarkable differences between the two structures in the orientations of the residues lining the pocket are observed (Figure 2).

The crystal structure of HSV-1 TK does not contain an ATP molecule. Instead, a sulfate ion is observed at the putative position of the β-phosphate of ATP.[7] This sulfate-binding site is located in close proximity to the 5′ hydroxyl function of thymidine (S···O5′ distance is 6.5 Å) and is coordinated by the side chains of Arg-222, Arg-163, Gln-221, and by the main-chain NH functions of Gly-59, Met-60, Gly-61, Lys-62, and Thr-63.[7]

The Substrates. The 5-substituted 2′-deoxyuridine substrates which have been used for the computational analysis, together with their affinities for the HSV-1 TK enzyme described in the literature,[8-10] are listed in Figure 3. Basically, the structures can be divided into two classes.

The first group involves 5-(thien-2-yl)-2′-deoxyuridine (**1**) as lead compound, with an IC_{50} value around 2 μM. Affinity for the enzyme is retained when the heterocyclic ring is connected *via* its 3-position (**8**), when the ring is replaced by an isothiazole (**7**), or when a halogen or methyl group is introduced at the 5 position of the 5-(thien-2-yl) ring (**2**, **5**, and **6**). In contrast, halogen substitutions at the 3-position of the thien-2-yl ring and the 4-position of the thien-3-yl ring decrease the affinity by approximately 1 order of magnitude (**3**, **4**, and **9**).

The second group includes 5-(furan-2-yl)-2′-deoxyuridine (**10**) as lead structure. As in the case of the thiophene compounds, affinity is retained when the furan ring is connected *via* its 3-position (**13**). However, in contrast to the thiophene derivatives, affinity decreases significantly when a halogen group is substituted at the 5-position of the furan-2-yl ring (**11** and **12**) or when the heterocyclic ring is replaced by an isoxazole (**14** and **15**).

Clearly, there is a difference between both classes of molecules. Crystal structure analysis revealed that all compounds have a quasi-coplanar geometry between the five-membered heterocyclic ring and the uracil base (Figure 4).[11-14] Intramolecular interactions stabilize this coplanarity. Interestingly, in the 2-thienyl series of compounds, coplanarity is stabilized by an interaction between the O4 carbonyl group of the uracil base and the sulfur atom of the thiophene ring (Figure 4, structure **A**). A similar orientation for the isothiazole derivative (Figure 4, structure **B**) has been deduced from its NMR spectrum[15] and quantum-chemical calculations, which predict a stability of 17 kJ/mol of the NMR observed orientation relative to the other possibility.[15] In contrast, the orientations of the 2-furanyl and isoxazolyl rings are clearly different from the thiophene

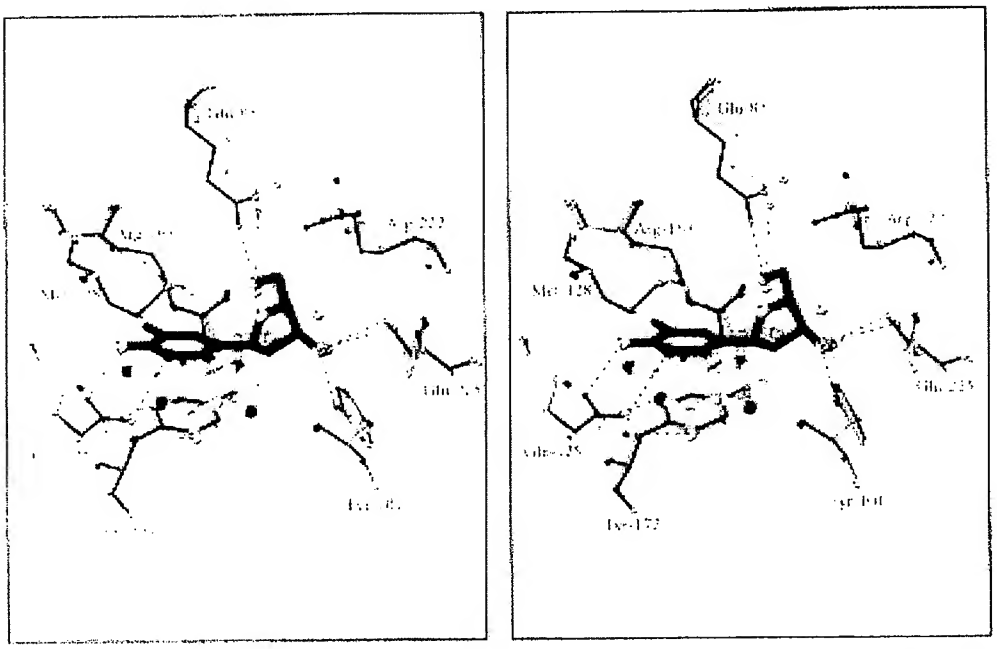

Figure 2. Stereoview comparing the binding modes of thymidine (dark gray bonds) and ganciclovir (light gray bonds) in the active site pocket of HSV-1 TK. Oxygen and nitrogen atoms are drawn as light and dark gray spheres, respectively. Hydrogen bonds are indicated as dashed lines. There is a remarkable overlap between the amino acid side chains in the two active site pockets. The only exception is Gln-125, whose amide functionality is flipped approximately 180° between the two crystal forms in order to optimize hydrogen bonding opportunities.

analogues, as they are stabilized by intramolecular interactions between the oxygen of the heterocycles and the H6 atom of the uracil base (Figures 4, structures **C** and **D**). The oxygens of the furanyl and isoxazolyl rings point therefore in an opposite direction compared to the sulfur atoms of the thienyl or isothiazolyl rings. The structures of the 3-thienyl and 3-furfuryl compounds are stabilized by an intramolecular contact between O4 of the uracil base and H2 of the heteroaromatic rings (Figure 4, structure **E**), which is analogous with the stabilizing O4···H6 interaction observed in the crystal structure of (*E*)-5-(bromovinyl)-2′-deoxyuridine (Figure 4, structure **F**).[16] Care was taken to maintain these specific conformations during the docking and energy minimization calculations by the use of appropriate torsion angle potentials.

The high structural similarity between the 17 5-substituted 2′-deoxyuridine analogues suggests that the loss of entropy upon binding the enzyme may be similar for all compounds. The 5-substituted uracil bases are planar, conjugated, and rigid systems, making them ideally suited for structure–affinity studies such as these.

Results

Binding of Thymidine. (A) Active Site Interactions. A stereoplot of the crystal structure with thymidine in the active site of HSV-1 TK is shown in Figure 2.[7] Three hydrogen bonds, involving the 3′- and 5′-hydroxyl groups of thymidine, link the sugar moiety of thymidine with the enzyme, while the nucleobase forms two hydrogen bonds through atoms N3 and O4. In addition to these hydrogen bond interactions, the uracil base is sandwiched or stacked between the C-methyl group of Met 128 on one side and the aromatic side chain of Tyr 172 along the other side. The 5-methyl group is located in a small hydrophobic pocket lined by residues of Tyr-132, Ala-167, Ala-168 (not shown), and the aliphatic side chain of Arg-163.

(B) Binding Energetics. A decomposition of the total binding energy of the minimized thymidine–HSV-1 TK complex on a per-residue basis or separated into individual contributions for the base and sugar part is listed in Table 1. Although the results are slightly dependent on the applied dielectric for calculating the interaction energies, the main conclusions remain the same. More than 80% of the total interaction energy comes from the interaction with only six residues, namely the four hydrogen bond partners Glu 83, Glu-225, Gln-125, Tyr-101, and residues Tyr-172 and Met 128, which sandwich the nucleoside base by means of stacking interactions. Thus, the major binding forces between thymidine and enzyme arise from hydrogen-bonding interactions involving the two hydroxyl groups on the sugar moiety and the amide function of the nucleobase, together with stacking interactions of the base plane. These conclusions are consistent with the decreased affinity of either ganciclovir ($IC_{50} = 50\ \mu M$),[17] where the purine base is less well stacked compared to thymidine, or acyclovir ($IC_{50} > 500\ \mu M$),[17] where only one hydroxyl function is available for hydrogen-bonding interactions.

Binding of 5-Substituted-2′-Deoxyuridine Substrates. (A) Exploration of Alternative Binding Modes for These Compounds. Considering the structural resemblance between the 5-substituted 2′-deoxyuridine analogues and thymidine, a binding conformation similar to the binding mode of thymidine seems reasonable at first sight. However, in principle, eight different binding modes are possible on paper, and these are shown in Figure 5.

The eight possible binding complexes are distinguished either by the side-chain conformation of Gln-125 (Table 2; compare binding modes **1a**, **1s**, **2a**, **2s** with

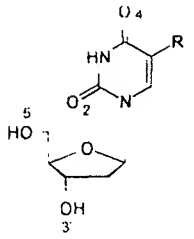

	R	C_{50} (μM)		R	C_{50} (μM)
1	Me	1.0	9		143
2		2.4	10		29
3		3.5	11		51
4		6.2	12		28
5		6.5	13		1.5
6		2.5	14		36
7		2.3	15		34
8		5.0	16		107
			17		0.3

Figure 3. The compounds with their numbering label and experimental affinity for HSV-1 thymidine kinase. Affinity data were obtained from literature[8,16] and are the concentrations required to inhibit thymidine phosphorylation by 50% against radiolabeled thymidine used at a concentration of 1 μM. All affinities were measured under the same conditions, and highly similar K_M values (0.25 μM) were found in all cases.[8]

3a, **3s**, **4a**, **4s**), by the orientation of the base with respect to sugar (*syn*/*anti* conformation; **1a**, **2a**, **3a**, **4a** *versus* **1s**, **2s**, **3s**, **4s**), and by the hydrogen-bonding pattern between the substrate base and the amide function of Gln-125 (**1a**, **1s**, **3a**, **3s** *vs* **2a**, **2s**, **4a**, **4s**).

However, although in principle eight different ways are feasible to dock 5-substituted substrates in the active site of HSV-1 TK, it is obvious that only a small fraction of these, if not only one, will be energetically feasible and will represent the "true" binding mode. Furthermore, since it has been shown that the 5′-hydroxyl functions of these substrates are phosphorylated to the same extent and in a similar way as the corresponding hydroxyl function of thymidine,[18] the true binding conformation will likely have its 5′-hydroxyl function in a similar orientation as found in the crystal structure of the thymidine (and ganciclovir) complex.[7]

In order to elucidate the most likely binding conformation from all the eight possibilities, we have docked and energy minimized model compound 5-(thien-2-yl)-2′-deoxyuridine (**1**) in the active site of HSV-1 TK and have subsequently evaluated each of the eight possible binding modes based on four criteria: (1) the number of hydrogen bonds between substrate and enzyme, (2)

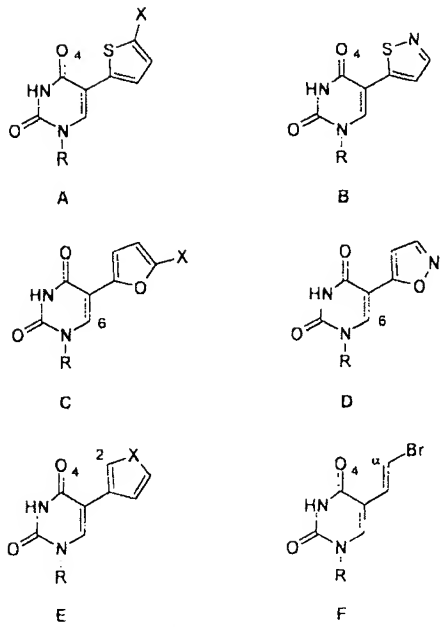

Figure 4. The crystal structure conformations of several 5-substituted 2′-deoxyuridine derivatives.

the root-mean-squared (rms) deviation of all active site residues from the corresponding minimized TK-thymidine positions, (3) the distance between sugar O5′ and sulfate S atoms, and (4) the interaction energy between substrate and enzyme. The results are summarized in Table 3. Minimized binding conformations **1a**, **2a**, **3a**, and **4a** of substrate **1** in the active site of HSV-1 TK are shown in Figure 6.

Following Table 3, we believe that the most likely or true binding conformation resembles binding mode **1a** for the following four reasons. First, in binding conformation **1a** we find that the distance between the sugar O5′ and sulfate S is closer than the corresponding distance to O3′. In fact, this is observed in all cases where an *anti*-orientation between base and sugar is adopted (Table 3, binding modes **1a**, **2a**, **3a**, **4a**). If the sulfate ion is indeed located near the putative binding site of the β-phosphate of ATP,[7] we might expect from these geometries that it is atom O5′ instead of atom O3′ which will get phosphorylated by the enzyme. This is in agreement with experiment.[18] On the contrary, exactly the opposite is found for the *syn*-oriented binding conformations (**1s**, **2s**, **3s**, **4s**), where phosphorylation of the O3′ atom is expected and therefore deviates from experiment[18] (Table 3).

Second, binding mode **1a** allows the formation of the maximum number of hydrogen bonds between substrate and enzyme, leading to a much tighter substrate binding compared to the other possibilities (Figure 6). For example, due to the different orientation of the substrate in binding modes **2a** and **3a** compared to **1a** and **4a**, hydrogen-bonding opportunities of the sugar O5′ atom with Glu-83 and the sugar O3′ with Glu-225 and Tyr-101 are lost in **2a** and **3a**. In conformation **2a** this loss is partially compensated by the formation of a new hydrogen bond between O3′ and Glu-83 (Figure 6). Additionally, while the docked conformation of **4a** prior to minimization was such that it allowed for the formation of two hydrogen bonds between the substrate base and Gln-125 (Figure 5), minimization however

Table 1. Decomposition of the Total Binding Energy for Thymidine and 5-(Thien-2-yl)-2′-deoxyuridine (1)[a]

	relative contribution to the total interaction energy (in %)[b]					
	thymidine			5-(thien-2-yl)-2′-deoxyuridine		
	r	2r	4r	r	2r	4r
	Residues within 5 Å of Substrate					
Glu 83	19	28	26	28		
Glu 225	18	20	18	18		
Glu 226	17	15	14	13		
Tyr 172	11	13	13	13		
Tyr 101	10	10	8	8		
Met 128	6	6	5	5		
Trp 88	1	3	6	5		
Arg 163	1	3	3	2		
His 58	3	1	5	4		
Ile 100	2	2	2	2		
Ile 97	2	1	1	1		
Ala 168	2	1	1	1		
Ala 167	1	2	4	4		
Tyr 132	1	1	4	4		
Gln 221	0	1	2	1		
Cys 129	0	0	0	0		
His 264	0	0	0	0		
Pro 166	0	0	1	0		
Arg 222	1	12	11	10		
	Substrate					
sugar moiety	55	53	48	45		
base moiety	30	12	35	36		
5-substituted group	5	5	17	19		

[a] All residues within 8 Å of the substrate and the substrate itself were allowed to relax. The remaining residues were kept constrained to their crystal structure coordinates using a harmonic force constant of 1000 kJ/mol·Å^2. Nonbonded interactions were calculated using a 10 Å cutoff distance. Either a distance dependent ($\varepsilon = r$) or a constant dielectric ($\varepsilon = 1$) was used for the calculation of electrostatic interactions. [b] The relative contribution to the total interaction energy for each residue is the interaction energy between the particular residue and the whole substrate, divided by the total interaction energy between all residues and whole substrate. The relative contribution to the total interaction energy for each substrate moiety is the interaction energy between the particular substrate moiety and the whole enzyme, divided by the total interaction energy between the whole substrate and the whole enzyme.

disrupts the hydrogen bond between the Nε2 atom of Gln-125 and the base O2 atom, as there is a tendency for this residue to flip back to its position as found in the crystal structure with thymidine (Figure 6).

Third, taking the natural substrate thymine as a reference, the least distortion is introduced in the residues lining the pocket when substrate is docked in a conformation resembling that of **1a**. This is evident from the rms deviation between the minimized TK − **1** and TK − thymidine complexes, calculated for all residues lining the active site pocket (Table 3). In contrast, the binding of 5-substituted 2′-deoxyuridine substrates in a conformation resembling binding modes **2a** or **3a** introduces several steric clashes with, for example, Tyr-101 (binding mode **2a**) and Arg-163 (binding modes **2a** and **3a**) (Figure 6).

Fourth, the interaction energy between substrate and enzyme is significantly more favorable when the substrate is docked in binding conformation **1a** compared to the other possibilities. This is likely the consequence of a more optimal complementarity (both steric and electrostatic) between enzyme and substrate when docked in this conformation. In the case of thymidine, more than 80% of the total interaction energy arises due to interactions of the sugar hydroxyl groups hydrogen bonded to Glu-83, Glu 225, and Tyr-101, and from the pyrimidine base which is stacked between Met-128 and Tyr-172, and hydrogen bonded to Gln-125 (Table 1). It is therefore no surprise that an alternative binding arrangement lacking one of these interactions may result in a significantly decreased interaction energy, and hence, affinity.

With Gln-125 in a conformation similar as in the thymidine complex:-

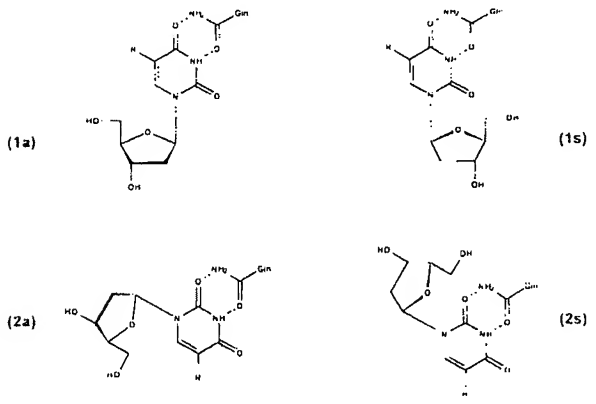

With Gln-125 in a conformation similar as in the ganciclovir complex:-

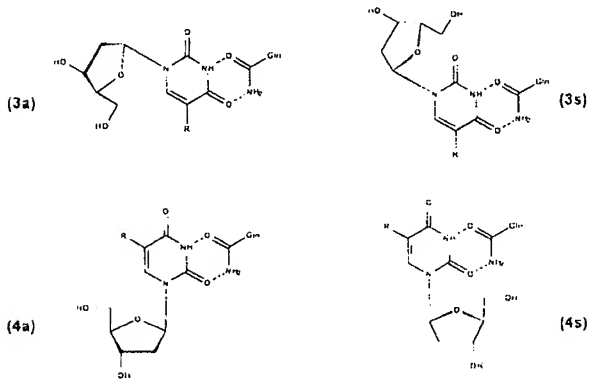

Figure 5. Eight possible binding orientations to dock a 5-substituted 2′-deoxyuridine substrate in the active site of HSV-1 TK. All orientations are drawn relative to the same fixed reference frame, *i.e.* the orientation of the active-site pocket is assumed to be similar in all eight cases. For a definition of -R, see Figure 3.

Table 2. Classification of the Possible Binding Conformations of the 5-Substituted 2′-Deoxyuridine Substrates by the Adopted Orientation of the Gln-125 Side Chain[a]

	binding mode	
	1a, 1s, 2a, 2s	3a, 3s, 4a, 4s
C Cα Cβ Cγ	162	176
Cα Cβ Cγ Cδ	56	56
Cβ Cγ Cδ Nε2	41 (resembling the values in the thymidine complex)	130 (resembling the values in the ganciclovir complex)

[a] Listed are the approximate starting values for the torsion angles of Gln-125 prior to energy minimization calculations (values in degrees).

(B) Binding Energetics of a Typical 5-Substituted Nucleoside: 5-(Thien-2-yl)-2′-deoxyuridine (1). A decomposition of the total binding energy for 5-(thien-2-yl)-2′-deoxyuridine (**1**) in binding conformation **1a** is

Table 3. Description of the Eight Possible Binding Conformations of 5-(Thien-2-yl)-2′-deoxyuridine (1) in the Active Site of HSV-1 TK[a]

binding mode	syn/anti[b]	HB	rms[c]	d(O5′···S)[d]	d(O3′···S)[e]	interaction energy[f] ε = 1	ε = r
1a	anti	5	0.1	7.0	8.8	316	311
1s	syn	3	0.7	12.0	7.8	259	250
2a	anti	5	1.1	7.6	8.0	228	187
2s	syn	3	0.9	11.2	7.8	224	213
3a	anti	2	0.8	9.1	11.8	244	234
3s	syn	1	0.8	11.8	8.1	255	211
4a	anti	4	0.5	6.6	8.7	292	297
4s	syn	3	0.9	11.8	7.8	242	239

[a] Described in terms of the number of hydrogen bonds between substrate and enzyme, the rms deviation of all active-site residues from their corresponding minimized TK···thymidine positions, the distance between sugar O5′ and O3′ atoms and sulfate S atoms, and the interaction energy. Each binding conformation was generated by manually docking substrate **1** in the required orientation followed by energy minimization until the gradient dropped below 0.01 kJ/mol·Å. A nonbonded cutoff of 10 Å in conjunction with a dielectric constant of $\varepsilon = 1$ or $\varepsilon = r$ was used. All residues within 8 Å of the substrate and the substrate itself were allowed to relax. The remaining residues were kept constrained to their crystal structure positions using a harmonic force constant of 100 kJ/mol·Å. [b] The reported number of hydrogen bonds, HB, rms deviations (rms), and distances between substrate hydroxyls and sulfate S [*d*(O5′···S) and *d*(O3′···S)] are from the minimized complexes calculated with a distance dependent dielectric ($\varepsilon = r$). Similar results were obtained using a constant dielectric ($\varepsilon = 1$) but are not shown for clarity. [c] The orientation of the substrate base moiety with respect to its sugar moiety. In the *syn* orientation, the base oxygen O2 is positioned above the sugar ring, while O2 is oriented away from the sugar ring in the *anti* conformation. [d] Number of hydrogen bonds between substrate and enzyme in the minimized complex. The definition of a hydrogen bond was solely based on distance criteria, *i.e.* the actual distance between the non-hydrogen atoms had to be smaller than the sum of the van der Waals radii (O, 1.4 Å; N, 1.55 Å). [e] The root mean squared distance in Å between the minimized TK-**1** and TK-thymidine complexes calculated for all residues within 3 Å of the substrate. [f] The distance in Å between the sugar O5′ and sulfate S atom. [g] The distance in Å between the sugar O3′ and sulfate S atom. [h] The interaction energy in kJ/mol between substrate and enzyme using two different dielectric constants ($\varepsilon = 1$ and $\varepsilon = r$).

given in Table 1. Very similar results were calculated for all other compounds of Figure 3 (data not shown). As in the case of thymidine, more than 80% of the total binding energy can be attributed to the sugar and nucleobase moieties. Strong hydrogen bonds between the sugar hydroxyls and residues Glu-83, Glu-225, and Tyr-101 and between the amide atoms N3 and O4 of the nucleobase and Gln-125, as well as base-stacking interactions, are responsible for this tight binding.

It is clear that substitution of the 5-methyl group of thymidine by a bulkier, unsaturated group such as a thiophene in **1** has no significant effect on the major binding interactions involving base and sugar moieties. Docking of 5-substituted 2′-deoxyuridine substrates in a conformation which resembles binding mode **1a** positions the 5-substituted group of the substrates in a small pocket where the 5-methyl group of thymidine is also bound. The major fraction of the solvent-accessible surface of this pocket is formed by Tyr-132. A molecular graphics exercise shows that only a small displacement of Tyr-132 is needed to enlarge this pocket such that it becomes large enough to occupy 5-substituted groups like thienyl moieties (Figure 7).

Understanding the Differences in Affinity of 5-Substituted 2′-Deoxyuridine Substrates: The Role of the 5-Substituted Side Chain. In an attempt to rationalize the observed affinity differences between the different 5-substituted substrates, a binding energy-affinity relationship study was undertaken. The 18 substrates listed in Figure 3 were alternatively docked in the active site of HSV-1 TK[7] in a binding conformation similar to **1a** (Figures 5 and 6), and their orientations were optimized by means of energy minimization techniques. Several energy calculations were performed for each substrate, each of them differing in the applied dielectric constant for calculating electrostatic interactions or in the number of enzyme residues that were allowed to relax. Interaction energies between substrate and enzyme, under the form of nonbonded van der Waals and electrostatic terms, were calculated for each complex and for each experimental setup to provide a measure of the tightness of binding. The results are listed in Table 4.

In order to account for possible differences in hydrophobicity between the compounds, free energies of solvation for each of the 18 substrates were also calculated. The electrostatic contribution to the total solvation free energy was calculated by solving the Poisson–Boltzmann equation.[19] The nonpolar component of the total solvation free energy was estimated from the solvent-accessible surface of each molecule.[20,21] It was assumed that the differences in solvation free energy between the 18 compounds could be largely attributed to the different substitution patterns at position 5. Therefore, to make the computations computationally feasible and to eliminate a possible dependency of the calculated solvation energy on the conformation of the sugar moiety, the whole 2′-deoxyuridine moiety was replaced by a methyl group. The results are listed in Table 5.

The correlation coefficients for the least squares fits between the logarithm of the IC_{50}'s and the calculated interaction energies, corrected for differences in hydrophobicity, are listed in Table 6. The best correlation is found for the case where the dielectric constant is treated as a distance-dependent function ($\varepsilon = r$) and where only the residues positioned within 3 Å of the substrate were allowed to relax. The least-squares equation for this particular case is given by

$$\ln(IC_{50}) = 0.177IE + \Delta G_{sol}/RT + 51.9, \qquad (1)$$

in which IE stands for interaction energy in kJ/mol, ΔG_{sol} is the solvation free energy of the substrate in kJ/mol, RT is expressed in kJ/mol, and IC_{50} is expressed in μM. Figure 8 shows a plot of this equation. It is clear from eq 1 that the affinity for this series of 5-substituted 2′-deoxyuridine substrates can be improved either by increasing the side chain's interaction energy (IE more negative) or by increasing the side chain's hydrophobicity (ΔG_{sol} more positive).

The interaction energies in eq 1 have been calculated without explicit solvent, using a distance-dependent dielectric and by allowing only part of the enzyme to minimize. It is therefore important to stress that both the slope and intercept of eq 1 have no real physical meaning, although in principle some contributions from, for example, enzyme desolvation, conformational entropy, and steric stress should be present. In principle, the equation could be expanded to include these factors as well. However, we have chosen not to do so, mainly

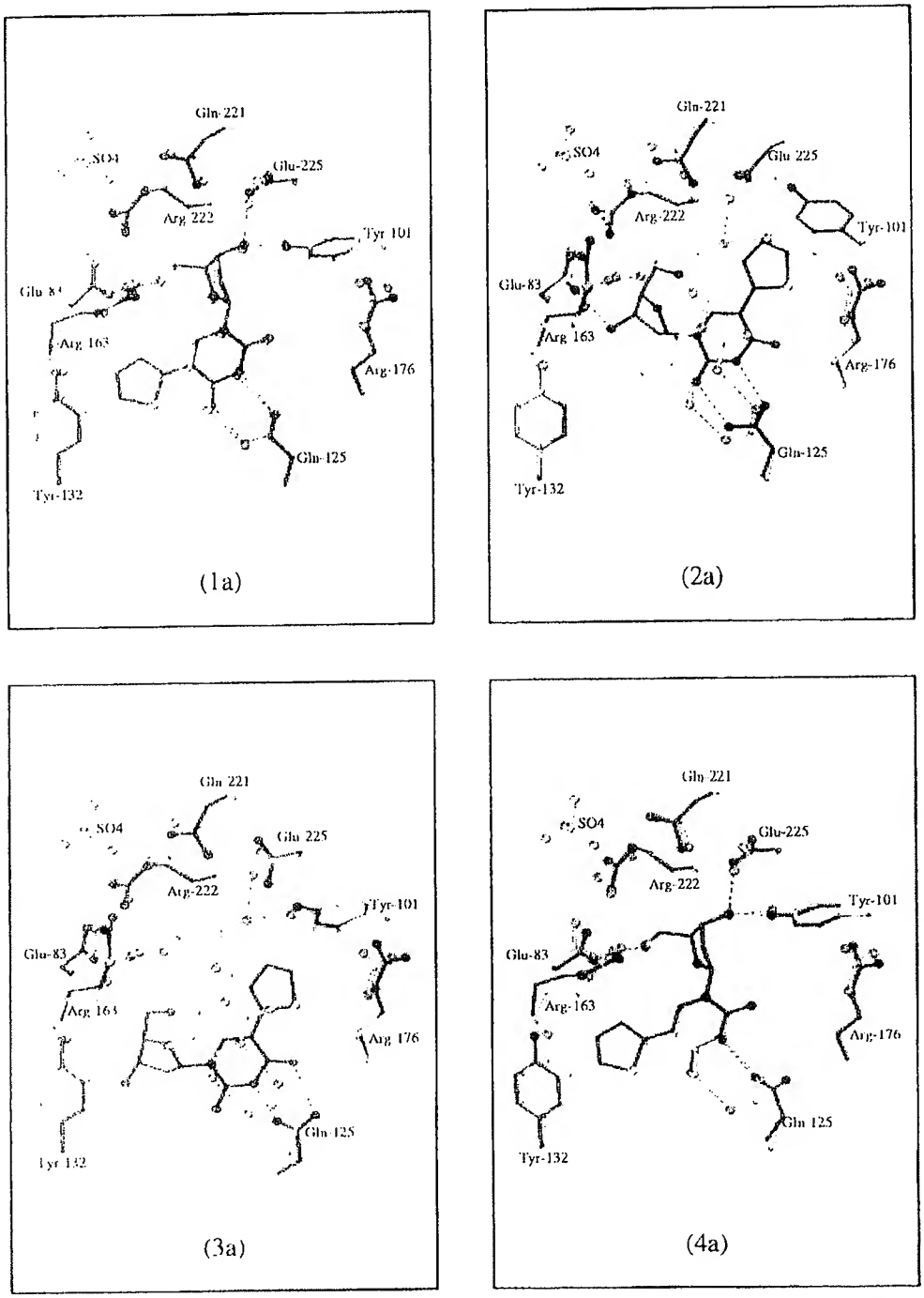

Figure 6. 5-(Thien-2-yl)-2′-deoxyuridine (**1**) energy minimized in the active site of HSV-1 TK. Four of the eight possible binding conformations are shown (**1a**, **2a**, **3a**, **4a**; Figure 5). Several residues lining the active-site pocket are also shown. The energy minimized complex between TK and thymidine (drawn using light-colored bonds) is shown as a reference. The substrate and its corresponding residues are drawn using dark-colored bonds. Hydrogen bonds are displayed as dashed lines.

because of difficulties in accurately estimating them and also because of the limited number of data to fit against.

Discussion

The Binding Conformation of 5-Substituted 2′-Deoxyuridine Substrates. On the basis of an exploration of the conformational space of 5-(thien-2-yl) 2′-deoxyuridine (**1**) in the active site of HSV-1 TK, we have found that the most likely binding conformation of these kind of substrates closely resembles that of thymidine (binding conformation **1a**, Figures 5 and 6). This is in accord with the observation that the affinities for the enzyme of many of these 5-substituted 2′-deoxyuridine substrates (Figure 3) are comparable with the corresponding value for thymidine. In this binding conformation the sugar hydroxyl groups are hydrogen bonded to Glu-83, Glu-225, and Tyr-101, and with the pyrimidine base stacked between Met-128 and Tyr-172, and hydrogen bonded to Gln-125. Together, these interactions represent more than 80% of the total interaction energy

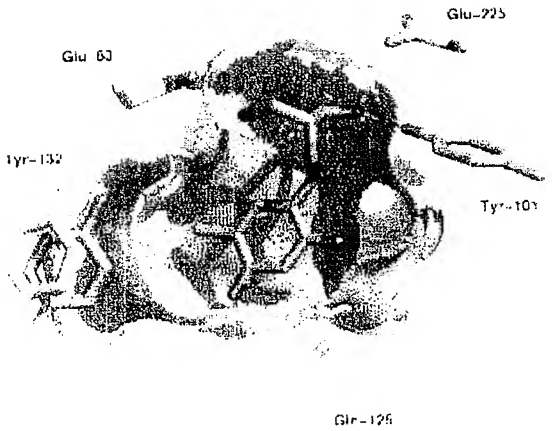

Figure 7. Only a minor small position shift of Tyr-132 is needed to enlarge the pocket of the 5-methyl group of thymidine so that it becomes large enough to occupy furane or thiophene groups. The yellow-colored part is the bottom part of the solvent accessible surface of the pocket as found in the crystal structure, colored in blue is the new pocket after a small position shift of Tyr 132.

Table 4. Calculated Interaction Energies (kJ/mol) between Substrate and HSV-1 TK Enzyme

	residue cutoff[a]					
substrate	1 Å	2 Å	3 Å	4 Å	6 Å	8 Å
	Constant Dielectric $\epsilon = 1$					
1	233	263	285	291	273	265
1	196	215	309	321	313	316
2	126	160	281	315	325	328
3	97	171	256	298	303	307
4	206	238	282	296	288	296
5	165	180	297	320	322	325
6	175	196	299	322	316	325
7	239	251	299	307	307	309
8	165	188	292	307	302	305
9	173	207	274	280	272	275
10	205	221	312	319	297	306
11	68	128	272	280	268	278
12	136	147	281	290	275	282
13	216	256	307	309	301	304
14	249	262	316	319	308	306
15	171	195	291	322	317	320
16	203	216	290	310	306	301
17	226	237	282	294	270	269
	Distance Dependent Dielectric $\epsilon = r$					
1	228	261	285	285	289	283
1	195	211	305	315	318	311
2	132	165	272	312	327	325
3	96	187	259	292	305	299
4	203	233	279	289	291	286
5	164	186	293	314	321	322
6	179	198	292	310	314	314
7	240	256	301	311	314	309
8	171	192	294	309	314	306
9	183	217	265	282	285	288
10	201	216	308	315	310	310
11	72	130	267	284	288	282
12	141	153	279	292	295	289
13	245	257	306	311	313	305
14	245	264	312	318	317	312
15	175	194	288	321	326	324
16	200	212	283	307	314	313
17	230	240	287	304	301	296

[a] All residues having at least one atom positioned within the cutoff distance of the substrate were allowed to relax. All other residues were kept constrained to their crystal structure coordinates using a harmonic force constant of 1000 kJ/mol·Å^2.

(Table 1), and it is therefore anticipated that an alternative binding arrangement lacking one of these interactions may result in a significantly decreased affinity, as is the case for, for example, acyclovir.[17]

Table 5. Calculated Solvation Free Energies ΔG_{sol} for Each of the 18 Compounds[a]

molecule	ΔG_{np}[b]	ΔG_{ele}	ΔG_{sol}
Me--CH_3	7.6	0.0	7.6
Me 1	9.7	-13.9	4.2
Me 2	10.9	-9.7	1.3
Me--3	11.8	5.0	6.7
Me 4	10.5	10.5	0.0
Me 5	10.5	10.9	0.4
Me 6	10.5	11.3	0.8
Me 7	9.7	21.0	11.3
Me 8	9.7	16.8	6.7
Me 9	10.9	11.8	0.8
Me 10	9.2	15.5	6.3
Me 11	10.5	10.5	0.0
Me 12	10.0	10.9	0.8
Me 13	9.2	15.5	6.3
Me 14	9.2	29.4	20.2
Me 15	10.0	20.6	10.5
Me 16	10.0	8.4	1.6
Me 17	9.2	-7.1	2.1

[a] ΔG_{np}, ΔG_{ele}, and ΔG_{sol} stands for nonpolar, electric, and total solvation free energy, respectively. Values are in kJ/mol. [b] Calculated from the solvent-accessible surface area (SAS) using $\Delta G_{np} = 4.7 + 0.046 \cdot (SAS)$. SAS in Å^2 and ΔG_{np} in kJ/mol.

Table 6. Correlation Coefficients r^2 for the Least-Squares Fits between the Logarithm of the IC_{50}'s and the Calculated Interaction Energies, with the Inclusion of Corrections for Differences in Hydrophobicity between the Compounds

	0 Å	2 Å	3 Å	4 Å	6 Å	8 Å
$\epsilon = 1$	0.3	0.2	0.7	0.3	0.1	0.1
$\epsilon = r$	0.4	0.2	0.8	0.6	0.3	0.2

The Role of the 5-Substituted Heterocyclic Group in Fine-Tuning the Affinity. The 5-substituted 2′-deoxyuridine analogues differ from the natural substrate thymidine only by the different substitution pattern at the 5-position. The spread in affinity of these compounds is narrow and ranges from 0.3 to 143 μM (Figure 3). It is likely that these small differences in affinity are the result of structural differences of the 5-substituted groups, and not from different binding conformations of the base or sugar moiety. Any structural changes with respect to these moieties would result in a much more drastic change in affinity, such as in the case of acyclovir which has an IC_{50} of more than 500 μM compared to 1 μM of thymidine.[17]

Equation 1 shows that, for this series of compounds, affinity for the enzyme is affected by both the hydrophobicity of the 5-substituted side chain and its interaction energy with the enzyme. According to this model, strong affinity results from the binding of hydrophobic compounds which are also characterized by their ability to interact strongly with the enzyme. Therefore, from the viewpoint of structure-based drug design, it may be of interest to investigate which geometric or electronic factors do influence either the interaction energies of the 5-substituted substrates or their hydrophobicities.

(A) Factors Influencing the Interaction Energy. (i) Steric Complementarity with the Active-Site Pocket. A general observation is that the interaction energy between substrate and enzyme decreases as the size of the thienyl of furanyl substituent increases (Table 4, distance dependent dielectric with 3 Å residue cutoff). Comparing, for example, the 2-thienyl ana-

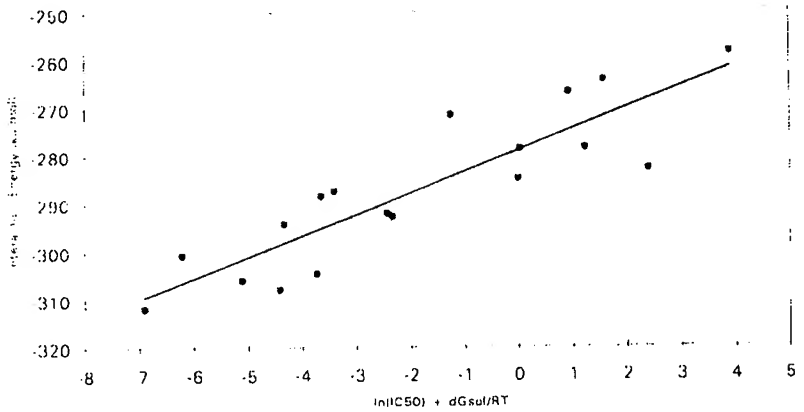

Figure 8. A plot of $\ln(IC_{50}) + \Delta G_{sol}/RT$ vs interaction energy.

logues, it is clear that the smaller, unsubstituted heterocyclic thiophene ring **1** fits the active-site pocket better than the larger, bromo-substituted thienyl compounds **2**–**4**. The same can be said for the substrates in the 2-furanyl series (**10** > **12** > **11**), or for the isoxazolyl series of compounds (**14** > **15**). Therefore, 5-substituted heterocyclic ring systems with small or no substitutions are preferred in terms of favorable interaction energy.

(ii) Electrostatic Complementarity with the Active-Site Pocket. The interaction energy of isoxazolyl **14** or furanyl derivative **10** is more favorable than the corresponding value of thiophene compound **1**. Figure 9 compares the predicted binding conformation of compound **14** with that of **1**. From this figure it can be seen that in the case of the isoxazole ring **14** a stabilizing interaction is formed due to the location of the two electronegative atoms O1 and N2 in a region of positive electrostatic potential. In the case of the thiophene ring **1** this stabilizing interaction is clearly absent because of the lack of any electronegative atoms in this region of positive potential. Thus, the introduction of electronegative atoms in the heterocyclic ring system at a position that allows them to interact with the positive potential at the back of the pocket may stabilize the interaction between substrate and enzyme to a certain extent.

(B) The Counterbalance between Hydrophobicity and Interaction Energy. In the case of 5-substituted 2′-deoxyuridine nucleosides, improved binding affinity for the enzyme can be obtained by ameliorating the compound's hydrophobicity by introducing halogen or methyl groups. However, the introduction of large groups onto the heterocyclic system often leads to a decrease in interaction energy with the enzyme. This in turn translates into decreased affinity so that the final affinity will remain somewhat unaffected. For example, Figure 3 shows there is no remarkable difference in measured affinity between the thiophene substrate **1** and its 2-methyl, 2-chlorine, or 2-bromine analogues (**6**, **5**, or **2**, respectively). However, introduction of a chlorine **12** or bromine atom **11** onto a furanyl ring **10** leads to a decrease in affinity of at least 1 order of magnitude. This is because the gain in affinity due to improved hydrophobicity of **11** and **12** is counterbalanced to a much larger extent by the loss of affinity due to the significant decrease in interaction energy as a consequence of steric clashes between the side chain of Arg 163 and the halogen substituent.

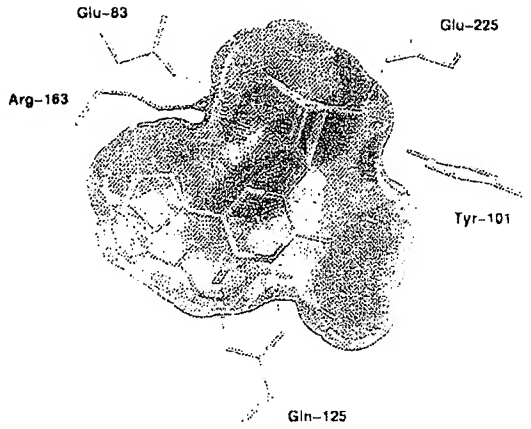

Figure 9. The electrostatic potential at the solvent-accessible surface of the active-site pocket. Red is positive potential; blue is negative. The C atoms of the isoxazole compound **19** are colored gray, and the thiophene analogue carbons **1** are colored cyan.

A similar conclusion can be drawn about the introduction of electronegative atoms in the five membered ring systems. Although the replacement of ring carbons with electronegative atoms often improves the interaction energy due to the favorable interaction with the positive electrostatic potential near the back of the pocket, the resulting structures are characterized by a decreased hydrophobicity. This is exemplified by comparing the affinities of the 2-furanyl substrate **10** with those the isoxazolyl compound **14**. The small gain in affinity due to the increased interaction energy of **14** compared to that of **10**, is completely counterbalanced by the significant loss of hydrophobicity of **14** compared to that of **10**.

It is clear that structural changes aimed at improving the 5 substituent's hydrophobicity are often counterbalanced by decreased interaction energies and *vice versa*. Therefore, for the design of improved 5-substituted 2′-deoxyuridine analogues, it is the drug designer's challenge to search for that molecule which forms the best compromise between hydrophobicity and structural complementarity to the enzyme.

Validating the Model. In order to assess the significance of the above derived correlation between interaction energy, hydrophobicity, and affinity (eq 1), its success in predicting the IC_{50} of 5-(pyrrol-1-yl)-2′-deoxyuridine (**18**) (Figure 10) was investigated. This

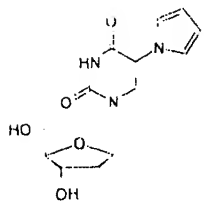

Figure 10. The structure of 5-(pyrrol-1-yl)-2′-deoxyuridine (**18**) used to validate the derived correlation between interaction energy, hydrophobicity, and affinity.

compound had already been synthesized before, but its affinity for HSV-1 TK had never been measured so far. 5-(Pyrrol-1-yl)-2′-deoxyuridine (**18**) was considered to be a suitable candidate because of its structural resemblance with compounds like those of Figure 3. A total solvation free energy for 1-methylpyrrole of −9.1 kJ/mol and, after docking compound **18** in the active site of HSV-1 TK, an interaction energy of −304 kJ/mol were calculated. Following eq 1, this corresponds to a predicted IC_{50} of 6 μM, which is in excellent agreement with a measured value of 7 μM.

Conclusion

Thymidine kinase from HSV-1 is a key enzyme in the metabolic activation of antiviral nucleosides. High affinity of these compounds for the enzyme is required for efficient phosphorylation. Recently, a new series of 5-substituted 2′-deoxyuridine nucleoside substrates as anti-HSV-1 agents has been discovered, and many of these compounds show high affinity for the viral TK enzyme. The availability of these data in combination with the recently solved structure of HSV-1 TK was an attractive opportunity to investigate the structural factors which would influence the affinity of these compounds for the enzyme.

Modeling calculations indicated that the binding energetics of thymidine and 5-substituted 2′-deoxyuridine analogues are very similar. The majority of the binding energy arises from hydrogen-bonding interactions involving sugar and base moieties. Stacking interactions of the uracil base contribute the remaining binding forces.

Calculations also indicated that the observed affinity differences of the 5-substituted nucleosides are fine-tuned by either the hydrophobicity of the 5-substituted side chain or its interaction energy with the enzyme. Hydrophobicity can be decreased by the introduction of halogen substituents, whereas the interaction energy can be improved by the introduction of electronegative atoms at well-defined positions, or by keeping the geometry of the five-membered heterocycle small. However, for this series of 5-substituted nucleosides, structural modifications aimed at improving the compound's hydrophobicity are often counterbalanced by decreased interaction energies, and *vice versa*, which makes the design of potent 5-substituted substrates an interesting challenge. The present study also explains why 5-(bromovinyl)-2′-deoxyuridine is one of the strongest binding compounds, and it, finally, gives a qualitative explanation for the first metabolic step in the activation of these class of compounds.

Experimental Section

The HSV-1 TK Crystal Structure. The crystal structure of HSV-1 TK in complex with thymidine was used as starting structure.[5] All crystallographic waters were removed. HB-PLUS[25] was used to provide an analysis of the hydrogen bonding pattern around the Asn, Gln, and His side chains and if necessary to exchange their N/O atoms where the hydrogen bonding pattern suggested it. Hydrogen atoms were added at geometrically reasonable positions using MacroModel.[26] Polar hydrogens of Ser, Tyr, and Thr residues were repositioned manually based on geometrical and hydrogen-bonding criteria. All His residues were assumed to be neutral. Geometrical and hydrogen-bonding criteria were used to decide between the two tautomeric configurations. Three His residues were modeled with their Nε atom protonated (58, 142, 213), and the other five His residues were protonated at Nδ (105, 164, 283, 323, and 351).

Charge and Force Field Parameter Development. The AMBER* force field[24] was used. Partial atomic charges for the substrates were calculated using the standard procedure of fitting the electrostatic potential at the STO-3G level of theory.[29] With the exception of torsion angle and some bond and angle parameters, all necessary parameters for the substrates were provided by the AMBER* force field. Missing bond and angle parameters were derived from comparison with the crystal structures, while their force constants were taken from comparable bonds or angles from the AMBER* force field. In cases where no torsion parameters were available, appropriate parameters were derived by comparison with torsion profiles calculated at the 6-31G* level of theory. However, because we were interested not in molecular dynamics but only in energy minimization calculations, little or no attempts were made to accurately model the height of barrier between local energy minima. A modified AMBER* force field file in MacroModel format containing partial charges and modified force field can be obtained from the authors upon request.

Energy Calculations. Energy calculations on enzyme-substrate complexes were performed using the BatchMin module of MacroModel 5.0.[26] No explicit waters or other approaches to model solvent were used because the substrates in the active-site pocket are totally shielded from bulk solvent. Furthermore, nearly all solvent-accessible residues were kept constrained to their crystal coordinates (see further), so that possible conformational changes due to the absence of solvent during the calculations were avoided. After the substrates were docked in the active site, the whole complex was energy minimized until the energy gradient dropped below 0.01 kJ/mol·Å. Other minimization protocols, such as simulated annealing procedures by which the systems were slowly cooled from 300 to 10 K over a 300 ps time scale, followed by energy minimization, did not improve the results to any extent (data not shown). Similarly, medium temperature molecular dynamics in conjunction with energy minimization to explore conformational space did not yield new binding conformations.[30] Either a distance-dependent or a constant dielectric was used to calculate electrostatic interactions using a non-bonded cutoff distance of 10 Å. Only part of the enzyme was allowed to relax, and residues further than a specified distance (0, 2, 3, 4, 6, or 8 Å) from the substrate were kept constrained to their crystallographic positions using a harmonic force constant of 1000 kJ/mol·Å^2.

Calculation of Solvation Free Energies. The electrostatic component of the total solvation free energy was calculated by solving the Poisson–Boltzmann equation[31] using a finite difference method as implemented by the DelPhi program.[20,22,23] The solvent-accessible surface was calculated with the DMS program of MidasPlus[27] using a probe radius of 1.4 and 0 Å for the solvent calculations (ϵ = 80) and vacuum (ϵ = 2) calculations, respectively. Partial atomic charges were obtained from 6-31G** calculations using the CHELPG procedure of GAMESS.[31] The reduced radii set of Sitkoff and coworkers was used for the atomic radii to calculate the solvent-accessible surface.[20] This procedure should guaranty the calculation of solvation energies with an average accuracy better than 3 kJ/mol.[20] Other charge sets, such as the STO-3G-derived atomic partial charges of the AMBER* force field, were also tried but yielded much less satisfying correlations (data not shown).

The nonpolar component of the total solvation free energy was estimated from the solvent accessible surface area using standard Pauling radii. A linear least squares relationship between the nonpolar component of the total solvation free energy and the solvent accessible surface area was calculated from experimental alkane transfer free energies,[24] and this least squares relation served to extrapolate the nonpolar solvation energies of the compounds under study.

Acknowledgment. Authors are indebted to all colleagues which contributed to this article by their skillful execution of all chemical, physical, biological, and biochemical experiments. Substrates were synthesized in our laboratory by P. Wigerinck, C. Pannecouque, I. Luyten, Liu Jie, A. Van Aerschot, and L. Kerremans. Antiviral data and HSV 1 TK affinities were measured by E. De Clercq and J. Balzarini at the Rega Institute of Leuven, Belgium. Small molecule crystal data were obtained from A. Olivier, C. Evrard, I. Creuven, and F. Durant at the University of Namur, Belgium.

References

(1) Prusoff, W. H.; Synthesis and biological activity of iododeoxyuridine and other halogenated pyrimidine nucleosides. *Biochim. Biophys. Acta* **1959**, *32*, 295–296.

(2) Herdewijn, P. A. M. M.; 5-Substituted 2′-deoxyuridines as anti HSV 1 agents: synthesis and structure activity relationship. *Antiviral Chem. Chemother.* **1994**, *5*, 131–146.

(3) De Clercq, E.; Descamps, J.; De Somer, P.; Barr, P. J.; Jones, A. S.; Walker, R. T. (*E*)-5-(2-Bromovinyl)-2′-deoxyuridine: a potent and selective anti herpes agent. *Proc. Natl. Acad. Sci. U.S.A.* **1979**, *76*, 2947–2951.

(4) Spadari, S.; Maga, G.; Focher, F.; Ciarrocchi, G.; Manservigi, R.; Arcamone, F.; Capobianco, M.; Carcuro, A.; Colonna, F.; Iotti, S.; Garbesi, A.; Thymidine is phosphorylated by herpes simplex virus type 1 thymidine kinase and inhibits viral growth. *J. Med. Chem.* **1992**, *35*, 1211–4220.

(5) Coen, D. M.; The implications of resistance to antiviral agents for herpes virus drug targets and drug therapy. *Antiviral Res.* **1991**, *15*, 287–300.

(6) Coen, D. M.; Kosz-Vnenchak, M.; Jacobson, J. G.; Leib, D. A.; Bogard, C. L.; Schaffer, P. A.; Tyler, K. L.; Knipe, D. M. Thymidine kinase-negative herpes simplex virus mutants establish latency in mouse trigeminal ganglia but do not reactivate. *Proc. Natl. Acad. Sci. U.S.A.* **1989**, *86*, 4736–4740.

(7) Brown, D. G.; Visse, R.; Sandhu, G.; Davies, A.; Rizkallah, P. J.; Melitz, C.; Summers, W. C.; Sanderson, M. R. Crystal structures of the thymidine kinase from herpes simplex virus type 1 in complex with deoxythymidine and Ganciclovir. *Nature Struct. Biol.* **1995**, *2*, 876–881.

(8) Wigerinck, P.; Pannecouque, C.; Snoeck, R.; Claes, P.; De Clercq, E.; Herdewijn, P. (*E*)-5-(2-Bromothien-2-yl)-2′-deoxyuridine and 5-(5-chlorothien-2-yl)-2′-deoxyuridine are equipotent to (*E*)-5-(2-bromovinyl)-2′-deoxyuridine in the inhibition of herpes simplex virus type 1 replication. *J. Med. Chem.* **1991**, *34*, 2383–2389.

(9) Wigerinck, P.; Snoeck, R.; Claes, P.; De Clercq, E.; Herdewijn, P. Synthesis and antiviral activity of 5-heteroaryl substituted-2′-deoxyuridines. *J. Med. Chem.* **1991**, *34*, 1767–1772.

(10) Wigerinck, P.; Kerremans, L.; Claes, P.; Snoeck, R.; Maudgal, P.; De Clercq, E.; Herdewijn, P. Synthesis and antiviral activity of 5-(thien-2-yl)-2′-deoxyuridine analogues. *J. Med. Chem.* **1993**, *36*, 3388–3395.

(11) Olivier, A.; Creuven, I.; Evrard, C.; Evrard, G.; Dorv, M.; Van Aerschot, A.; Wigerinck, P.; Herdewijn, P.; Durant, F. Stereoelectronic properties of five anti-HSV 1 2′ deoxynucleosides analogues with heterocyclic substituents in the 5-position: A comparison with BVDU. *Antiviral Res.* **1994**, *24*, 289–304.

(12) Creuven, I.; Evrard, C.; Evrard, G.; Wigerinck, P.; Herdewijn, P.; Durant, F. Relationship between structural properties and affinity for HSV 1 kinase of bromine substituted 5 heteroaromatic 2′ deoxyuridines. *Antiviral Res.* **1996**, *30*, 63–74.

(13) Creuven, I.; Evrard, C.; Evrard, G.; Wigerinck, P.; Herdewijn, P.; Durant, F. Crystal structure of 5 (thien 2 yl)uracil analogues: 5-(5-methylthien-2-yl)-2′-deoxyuridine, 5 (5-chlorothien-2-yl)-2′-deoxyuridine and 5-(5-bromothien-2 yl)-2′-deoxyuridine. *J. Chem. Cryst.*, in press.

(14) Creuven, I.; Lebon, F.; Busson, R.; Herdewijn, P.; Durant, F. Structural study of two 5-heteroaromatic 2′-deoxyuridines and their bromine analogues: theoretical conformational analysis and NMR experiments. Manuscript in preparation.

(15) Luyten, I.; De Winter, H.; Busson, R.; Lescrinier, L.; Creuven, I.; Durant, F.; Balzarini, J.; De Clercq, E.; Herdewijn, P. Synthesis of 5 (isothiazol 5 yl) 2′ deoxyuridine and its interaction with the HSV 1 thymidine kinase. *Helv. Chim. Acta* **1996**, in press.

(16) Parkanyi, L.; Kalman, A.; Czugler, M.; Kuvacs, F.; Walker, R. T. A comparison of the conformations adopted by some 5 bromovinyl 2′ deoxyuridines and a correlation with their antiviral properties: an X-ray study. *Nucleic Acids Res.* **1987**, *15*, 4111–4121.

(17) Balzarini, J.; Bohman, C.; De Clercq, E. Differential mechanism of cytostatic effect of (*E*)-5-(2-bromovinyl) 2′-deoxyuridine, 9 (1,3 dihydroxy-2-propoxymethyl)guanine, and other antiherpetic drugs on tumor cells transfected by the thymidine kinase gene of Herpes Simplex virus type 1 or type 2. *J. Biol. Chem.* **1993**, *268*, 6332–6337.

(18) Bohman, C.; Balzarini, J.; Wigerinck, P.; Van Aerschot, A.; Herdewijn, P.; De Clercq, E. Mechanism of cytostatic action of novel 5 (thien 2 yl) and 5-(furan 2 yl) substituted pyrimidine nucleoside analogues against tumor cells transfected by the thymidine kinase gene of Herpes Simplex virus. *J. Biol. Chem.* **1994**, *269*, 8036–8043.

(19) Davis, M. E.; McCammon, J. A. Electrostatics in biomolecular structure and dynamics. *Chem. Rev.* **1990**, *90*, 509–521.

(20) Sitkoff, D.; Sharp, K. A.; Honig, B. Accurate calculation of hydration free energies using macroscopic solvent models. *J. Phys. Chem.* **1994**, *98*, 1978–1988.

(21) Ben-Naim, A.; Marcus, Y. Solvation thermodynamics of nonionic solutes. *J. Chem. Phys.* **1984**, *81*, 2016–2027.

(22) Honig, B.; Gilson, M. K. Calculation of the total electrostatic energy of a macromolecular system: solvation energies, binding energies, and conformational analysis. *Proteins* **1988**, *4*, 7–18.

(23) Honig, B.; Sharp, K.; Yang, A.-S. Macroscopic models of aqueous solutions: biological and chemical applications. *J. Phys. Chem.* **1993**, *97*, 1101–1109.

(24) Weiner, S. J.; Kollman, P. A.; Nguyen, D. T.; Case, D. A. An all atom force field for simulations of proteins and nucleic acids. *J. Comput. Chem.* **1986**, *7*, 230–252.

(25) McDonald, I. K.; Thornton, J. M. Satisfying hydrogen bonding potential in proteins. *J. Mol. Biol.* **1994**, *238*, 777–793.

(26) Mohamadi, F.; Richards, N. G. J.; Guida, W. C.; Liskamp, R.; Lipton, M.; Caufield, C.; Chang, G.; Hendrickson, T.; Still, W. C. MacroModel—An integrated software system for modeling organic and bioorganic molecules using molecular mechanics. *J. Comput. Chem.* **1990**, *11*, 440.

(27) Perrin, T. F.; Huang, C. C.; Jarvis, I. E.; Langridge, R. The MIDAS display system. *J. Mol. Graph.* **1988**, *6*, 13–27.

(28) Kraulis, P. MOLSCRIPT: a program to produce both detailed and schematic plots of protein structures. *J. Appl. Crystallogr.* **1991**, *24*, 946–950.

(29) Singh, U. C.; Kollman, P. A. An approach to computing electrostatic charges for molecules. *J. Comput. Chem.* **1984**, *5*, 129–145.

(30) De Winter, H. L.; von Itzstein, M. Aldose reductase as a target for drug design: molecular modeling calculations on the binding of acyclic sugar substrates to the enzyme. *Biochemistry* **1995**, *34*, 8299–8308.

(31) Schmidt, M. W.; Baldridge, K. K.; Boatz, J. A.; Elbert, S. T.; Gordon, M. S.; Jensen, J. H.; Koseki, S.; Matsunaga, N.; Nguyen, K. A.; Su, S.; Windus, T. L.; Dupuis, M.; Montgomery, J. A. General atomic and molecular electronic structure system. *J. Comput. Chem.* **1993**, *14*, 1347–1363.

JM960278V